Supplementary Information (SI) for Dalton Transactions.
This journal is © The Royal Society of Chemistry 2024

A Sulfur-Templated Ni-Ni' Coordination Polymer that Relies on a Polarizable Nickel Nitrosyl Hub

Manish Jana,[a] Prof. Michael B. Hall*[a] and Prof. Marcetta Y. Darensbourg*[a]

Department of Chemistry, Texas A & M University, College Station, Texas 77843, United States

Email: hall@science.tamu.edu, marcetta@chem.tamu.edu

Supporting Information

Table of Contents **Page No**

Experimental Section:

S1.1 ***Methods and Materials.*** All reactions and manipulations were performed either under inert atmosphere N_2 glove box or using standard Schlenk-line and syringe/rubber septa techniques under N_2 atmosphere. Dry solvents were purified and degassed via a Bruker solvent system. Reagents were purchased from commercial sources and used as received. The known compounds $[Ni(NO)(Cl)(PPh_3)_2]$[13], $[Ni(NO)(N_3)(PPh_3)_2]$[17] and $(dadt^{Bz})Ni$[16] were synthesized following the literature reported procedures.

S1.2 Physical measurements. Solution and solid infrared spectra were recorded on a Bruker Tensor 37 Fourier transform IR (FTIR) spectrometer in CaF_2 solution cell with a 0.2 mm path length and as thin films, respectively. ^1H spectra was recorded using the Bruker Avance NEO 400 MHz system with an automated tuning 5mm broadband iProbe (Acend magnet). Electrospray ionization mass spectrometry (ESI-MS) was performed by the Laboratory for Biological Mass Spectrometry at Texas A&M University.

Single crystal X-ray diffraction measurements were carried out at a low temperature employing a (three circle or kappa) Bruker-AXS (Quest or Venture) with IμS source and a Photon III area detector diffractometer for (Mo Kα radiation, λ = 0.71073 Å or Cu Kα radiation, λ = 1.54178 Å) (NSF-CHE-9807975, NSF-CHE-0079822 and NSF-CHE-0215838). Crystals (for color, habit, size see corresponding CIF files) were mounted on a nylon or Kapton® loops and cooled in a cold nitrogen stream (OXFORD Cryosystems (700 or 800), to 110(2) K. Bruker AXS APEX 3[29] software was used for data collection and reduction. Absorption corrections were applied using SADABS.[30] Space group assignments were determined by examination of systematic absences, E-statistics, and successive refinement of the structures. Structures were solved using SHELXT[31] and refined by least-squares refinement on F^2 followed by difference Fourier synthesis (OLEX2, SHELXL).[32,33] All hydrogen atoms were included in the final structure factor calculation at idealized positions and were allowed to ride on the neighboring atoms with relative isotropic displacement coefficients. Thermal parameters were refined anisotropically for all non-hydrogen atoms to convergence. The MERCURY 2022.1.0[34] interface was used for structure visualization, analysis of bond distances and angles, and drawing ORTEP plots. OLEX2[33] interface was used for structure overlay.

S1.3 Cyclic Voltammetry. Cyclic voltammograms were recorded on a CHI600E electrochemical analyzer (HCH instruments, Inc.). All experiments were performed under an Ar blanket in CH_3CN or DMF solutions containing a 0.1 M $[^nBu_4N][PF_6]$ electrolyte and 2.0 mM analyte at room temperature. A 0.071 cm^2 glassy carbon disk was used as the working electrode, platinum wire as the counter electrode, and $Ag^0/AgCl$ as the reference electrode. All potentials were referenced to the Fc/Fc^+ couple at 0.00 V.

Reaction of Ni(dadt^{Bz}) with $NiCl_2(PPh_3)_2$. Under inert atmosphere glove box, 86.12 mg (0.2 mmol) of $(dadt^{Bz})Ni$ was taken in a 20mL scintillation vial and a suspension of $NiCl_2(PPh_3)_2$ 131 mg (0.2 mmol) in 5 mL of MeOH was added to it and the vial was capped. The reaction was allowed to stir overnight at room temperature. After stirring overnight, the reaction mixture was filtered through celite and the filtrate was evaporated to dryness. The solid obtained was redissolved in minimum volume of acetonitrile and

filtered. The filtrate was layered carefully with ether at room temperature to result in metallic dark brown coloured blocks after two days. Yield = 30%.

Preparation of complex 1. Within an inert atmosphere glove box, 80 mg (0.199 mmol) of ($dadt^{Bz}$)Ni complex was taken in a 20mL scintillation vial and a suspension of $[Ni(NO)Cl(PPh_3)_2]$ 129.35 mg (0.199 mmol) in 5 mL of MeOH was added to it and the vial was capped. The reaction was stirred for 2h at room temperature. After completion of the reaction (monitored by IR), the reaction mixture was filtered through celite and the filtrate was evaporated to dryness. The solid obtained was washed with pentane multiple times to remove PPh_3 from the reaction mixture. *(If the complex is not properly washed with pentane, triphenylphosphine bound complex was observed in the mass spec)*. The dark blue colour solid was redissolved in minimum volume of acetonitrile and filtered. The filtrate was layered carefully with ether at −35°C to result in metallic dark green coloured blocks after two days. Yield = 95 mg (85%).

Elemental Analysis for complex **1** ($C_{21}H_{28}ClN_3Ni_2OS_2$)

Element	Calculated	Obtained	
C	45.41%	45.73%	45.91%
H	5.08%	5.15%	5.33%
N	7.57%	7.33%	7.47%

Note: The reaction was attempted in various solvents such as MeCN, MeOH as well as DCM. Although both the starting materials were initially partially soluble in MeOH, it has produced the clean product (monitored by IR). The first filtration step is also important as it will remove the unreacted starting materials from the reaction.

Preparation of complex 2.

*(**Caution!** Azide complexes are potentially explosive. The experiments mentioned here were carried out under inert atmosphere. Only a small amount of the materials should be prepared and those should be handled with great care.)*

Under inert atmosphere glove box, 95 mg (0.17 mmol) of Complex **1** was dissolved in 5 mL of MeOH in a 20 mL scintillation vial and 11 mg (0.17 mmol) of solid NaN_3 was added to it and the vial was capped. The reaction was stirred for 2h at room temperature. After completion of the reaction (monitored by IR), the reaction mixture was filtered through celite, and the filtrate was evaporated to dryness under a gentle flow of nitrogen. The dark blue colour solid was redissolved in a minimum volume of acetonitrile and filtered. The filtrate was layered carefully with ether at room temperature to result in metallic dark greenish-brown coloured needles after two days. Yield = 67 mg (70%).

Elemental Analysis for complex 2: $C_{21}H_{28}N_6Ni_2OS_2$

Element	Calculated	Experimental	
C	44.88%	45.23%	45.31%
H	5.02%	5.40%	5.32%
N	14.95%	14.66%	14.64%

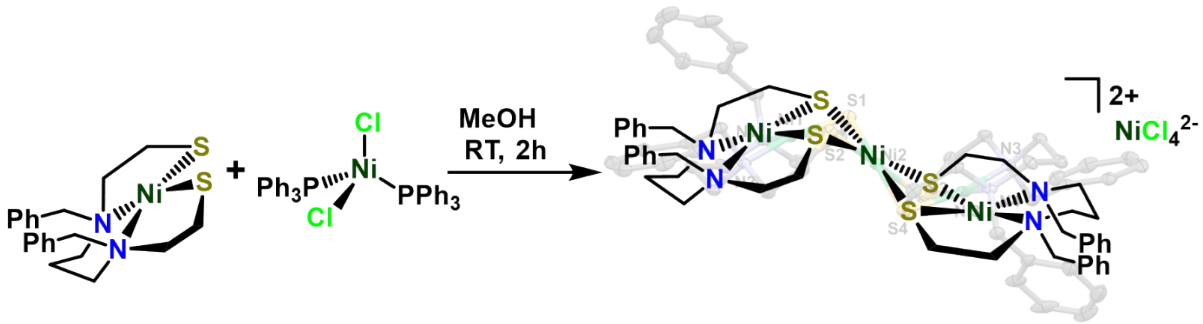

Scheme S1. Reaction of (dadtBz)Ni complex with $NiCl_2(PPh_3)_2$ in MeOH at room temperature.

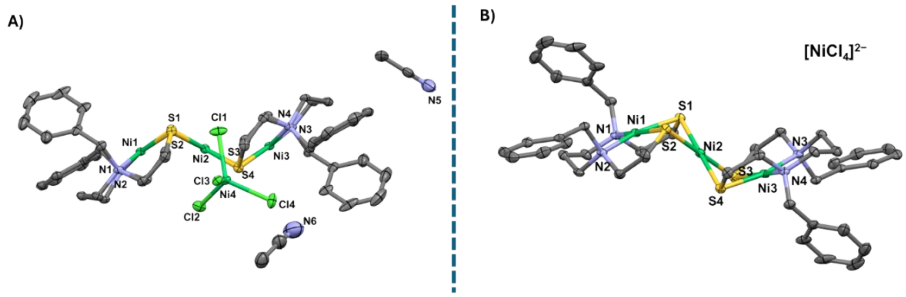

Figure S1. Crystal structure of trimetallic $[(dadt^{Bz})Ni•Ni•Ni(dadt^{Bz})]^{2+}[NiCl4]^{2-}$ complex.

Table S1. Selected bond distances and angles for the trimetallic complex.

BOND DISTANCES (Å)		BOND ANGLES (°)	
Ni1-N1	1.986	∠S1-Ni1-S2	80.55
Ni1-N2	1.991	∠S1-Ni2-S2	79.56
Ni1-S1	2.178	[b]Hinge Angle	114.03
Ni1-S2	2.164		
Ni2-S1	2.194		
Ni2-S2	2.194		
Ni3-N3	1.991		
Ni3-N4	1.986		
Ni3-S3	2.164		
Ni3-S4	2.178		
Ni1-Ni2	2.858		
Ni1-Ni3	5.716		
[a]Ni_{disp}	0.102		

[a]*D*isplacement from the mean N_2S_2 plane; [b]Hinge Angle is the angle between the NiN_2S_2 and the NiS_4 planes.

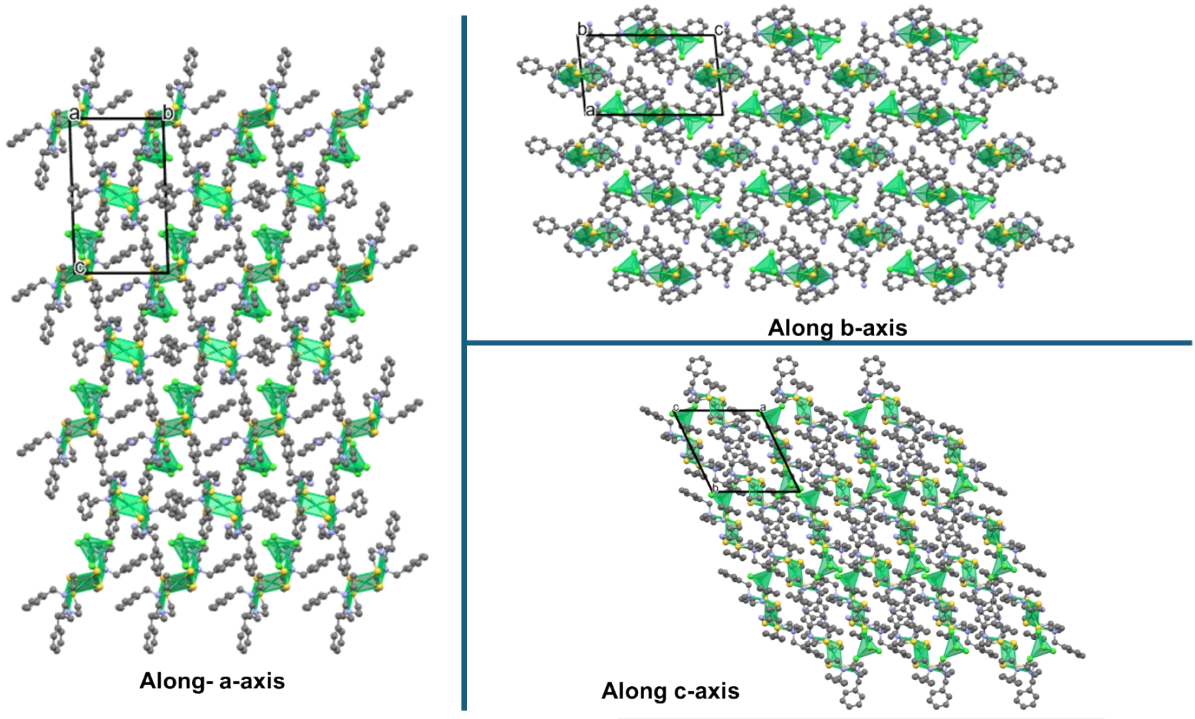

Figure S2. Crystal packing diagram for the trimetallic complex along three crystallographic axes.

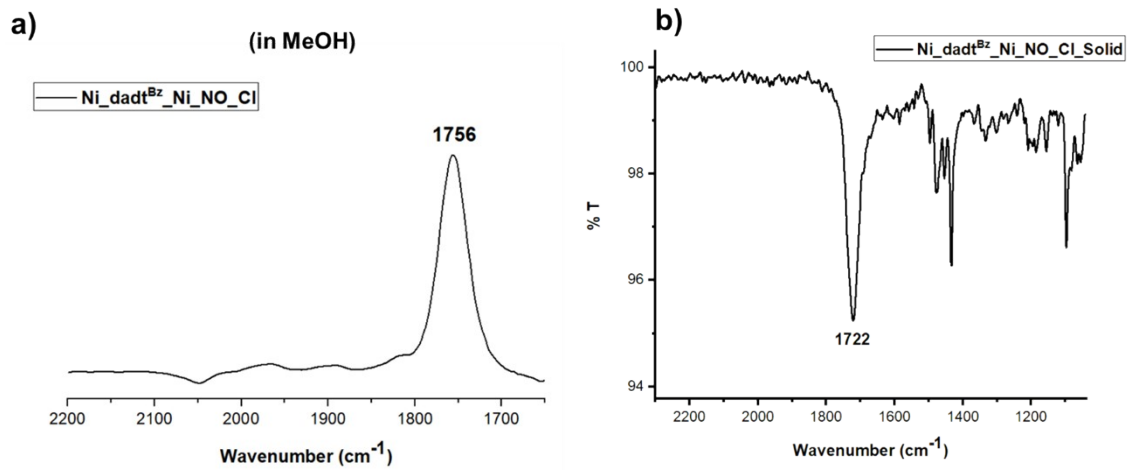

Figure S3. ν(NO) (a) solution (in MeOH) and (b) solid IR spectra of complex 1.

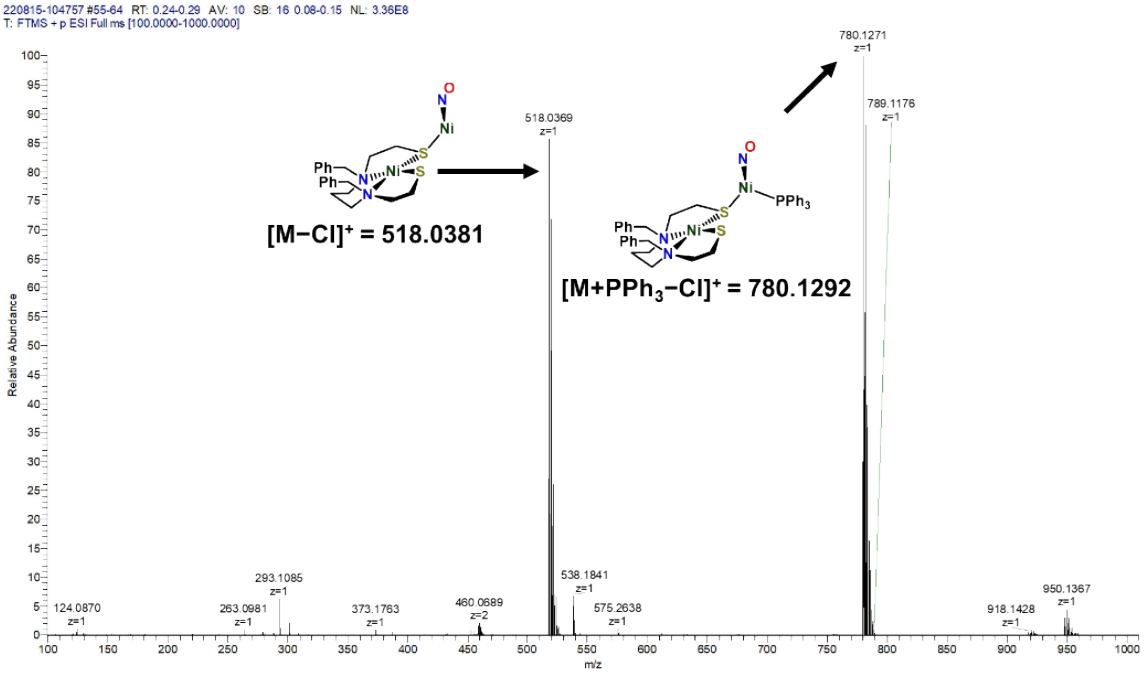

Figure S4. ESI-MS for complex 1 in MeOH. The peak at m/z = 780.1271 corresponds to the $[(M+PPh_3)-(Cl)]^+$ species. The peak at m/z = 518.0369 corresponds to $[M—Cl]^+$ species.

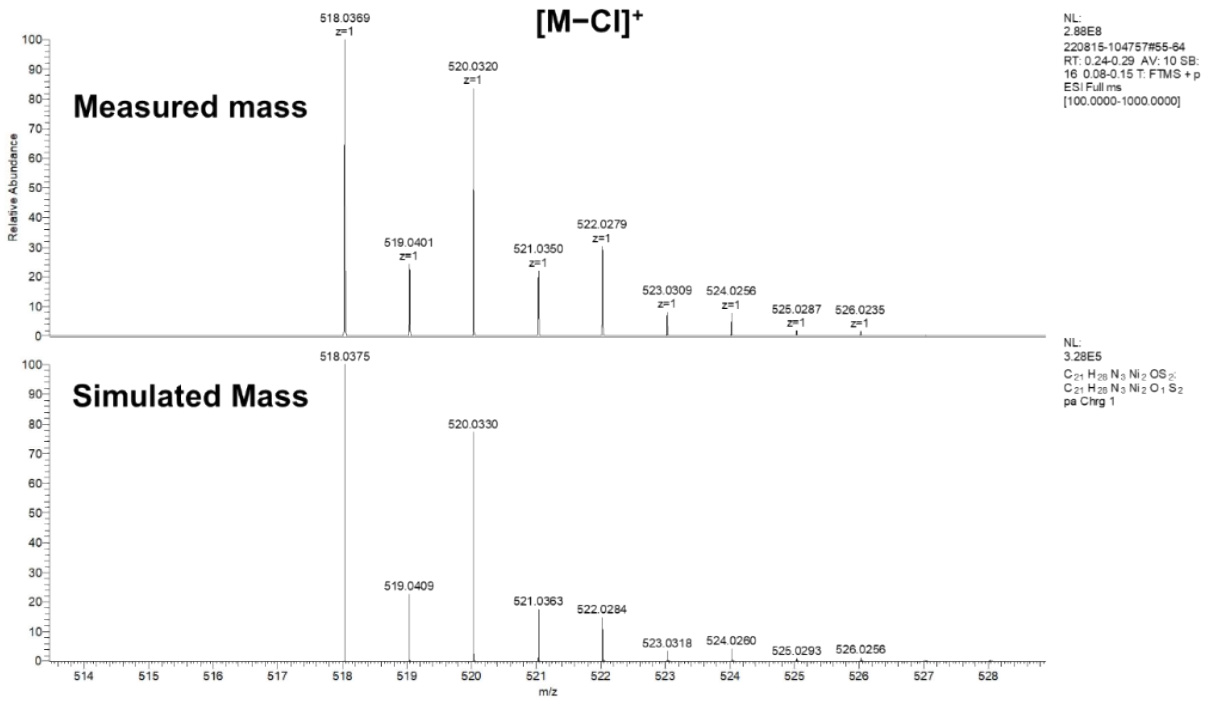

Figure S5. The experimental and simulated mass spectrum at m/z = 518.0369.

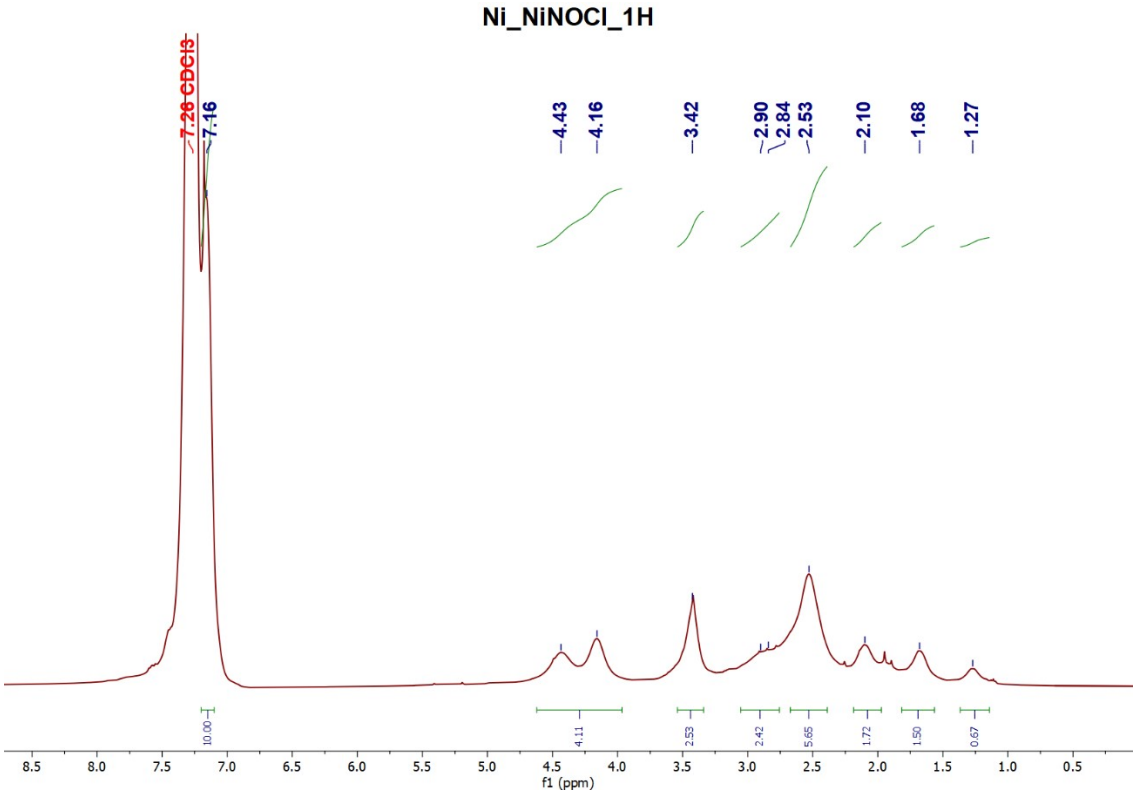

Figure S6. ^{1}H NMR of Complex 1 shows broad signals in $CDCl_3$ (400 MHz).

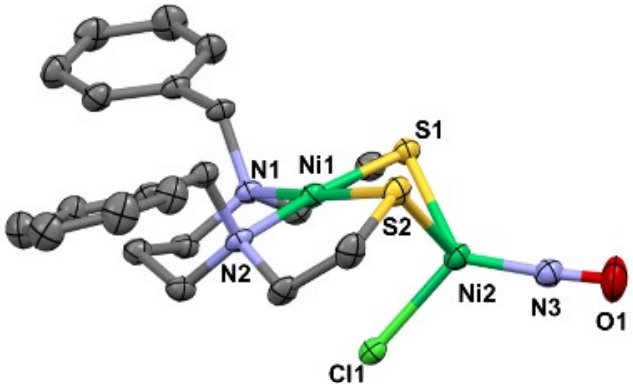

Figure S7. Single crystal x-ray structure for complex 1.

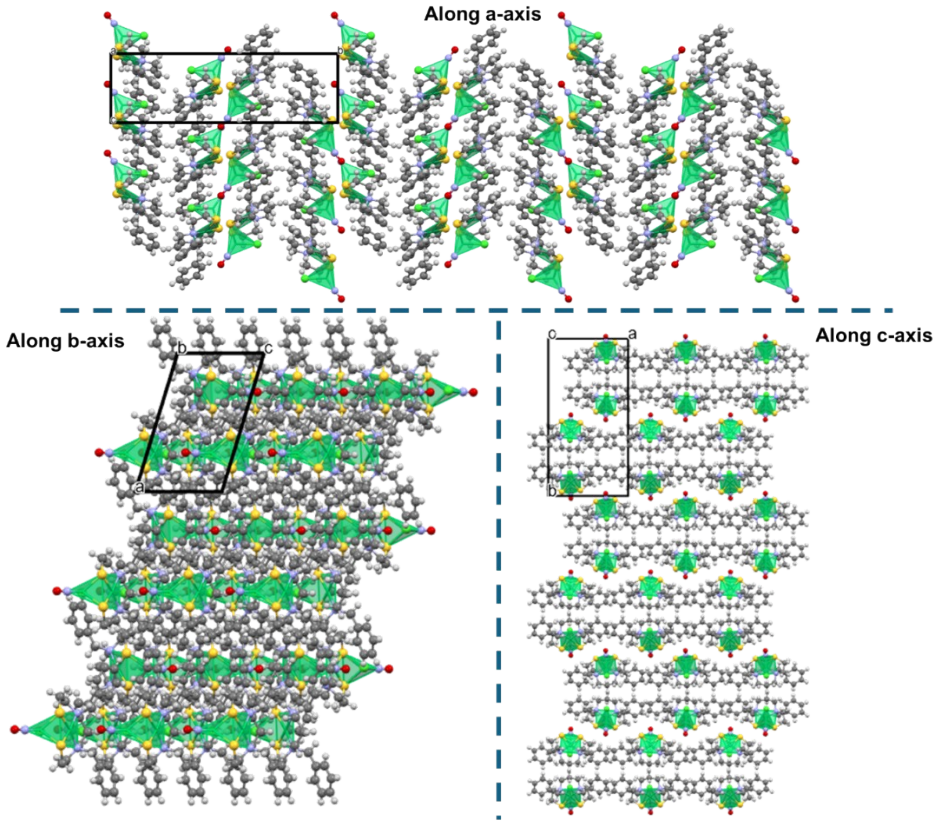

Figure S8. Crystal packing diagram for complex 1 along 3 crystallographic axes. The green polyhedral corresponds to the nickel centers.

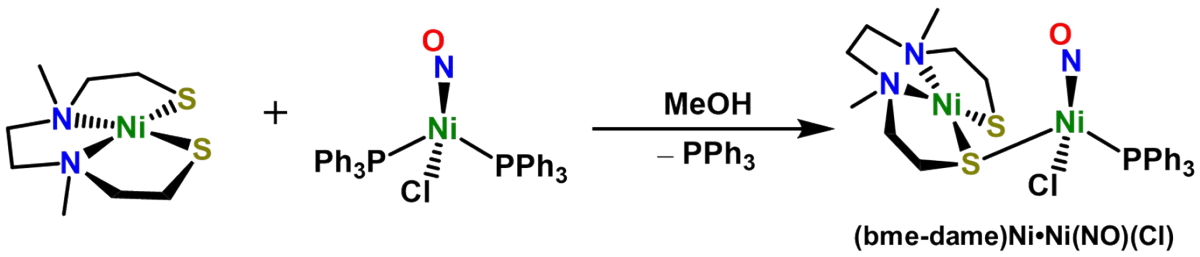

Scheme S2. Reaction of (bme-dame)Ni with [Ni(NO)(Cl)(PPh_3)$_2$] in MeOH. The crystals suitable for x-ray diffraction were obtained by layering acetonitrile with ether.

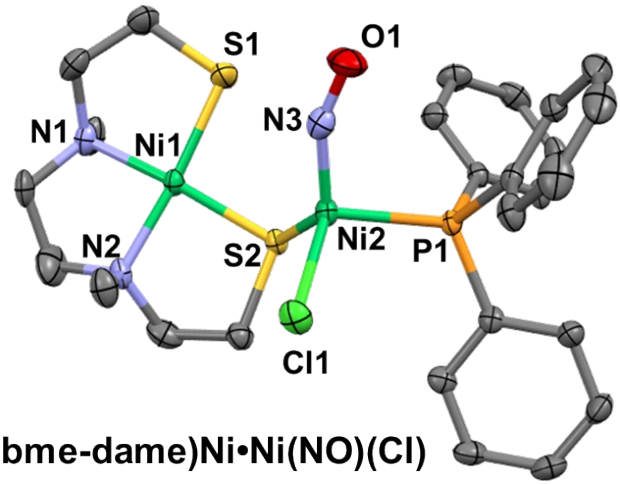

(bme-dame)Ni•Ni(NO)(Cl)

Bond Distances (Å)		Bond Angles (°)	
Ni1—Ni2	3.655	∠Ni2-N3-O1	154.13
Ni2—Cl1	2.28	∠S1-Ni1-S2	94.93
Ni2—P1	2.23	∠S2-Ni2-P1	101.81
Ni2—S1	3.874		
Ni2—S2	2.331		
Ni2—N3	1.670		
N3—O1	1.174		

Figure S9. Single crystal x-ray structure of [(bme-dame)Ni•Ni(NO)(Cl)(PPh_3)] complex. Selected bond distances and angles are shown in the table.

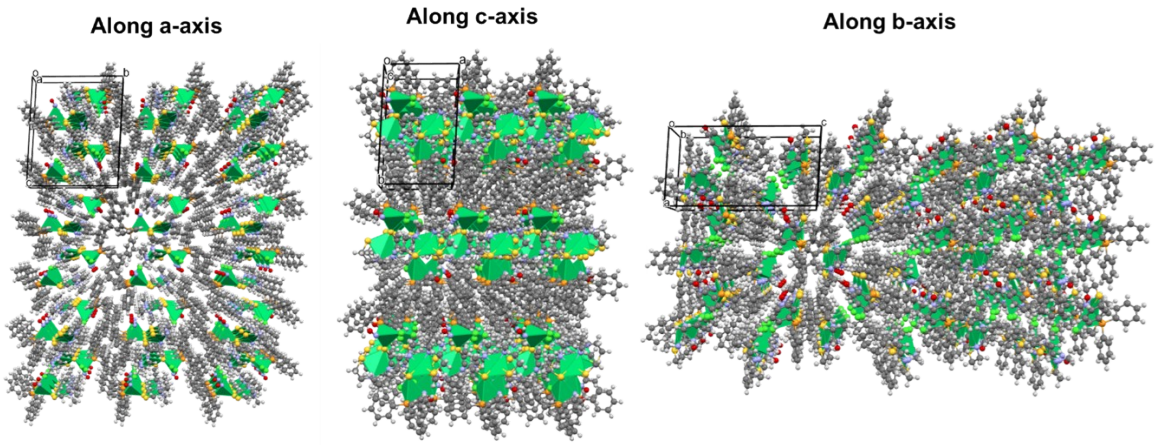

Figure S10. Crystal packing diagram for [(bme-dame)Ni•Ni(NO)(Cl)(PPh_3)] complex along 3 crystallographic axes. The green polyhedral corresponds to the nickel centers.

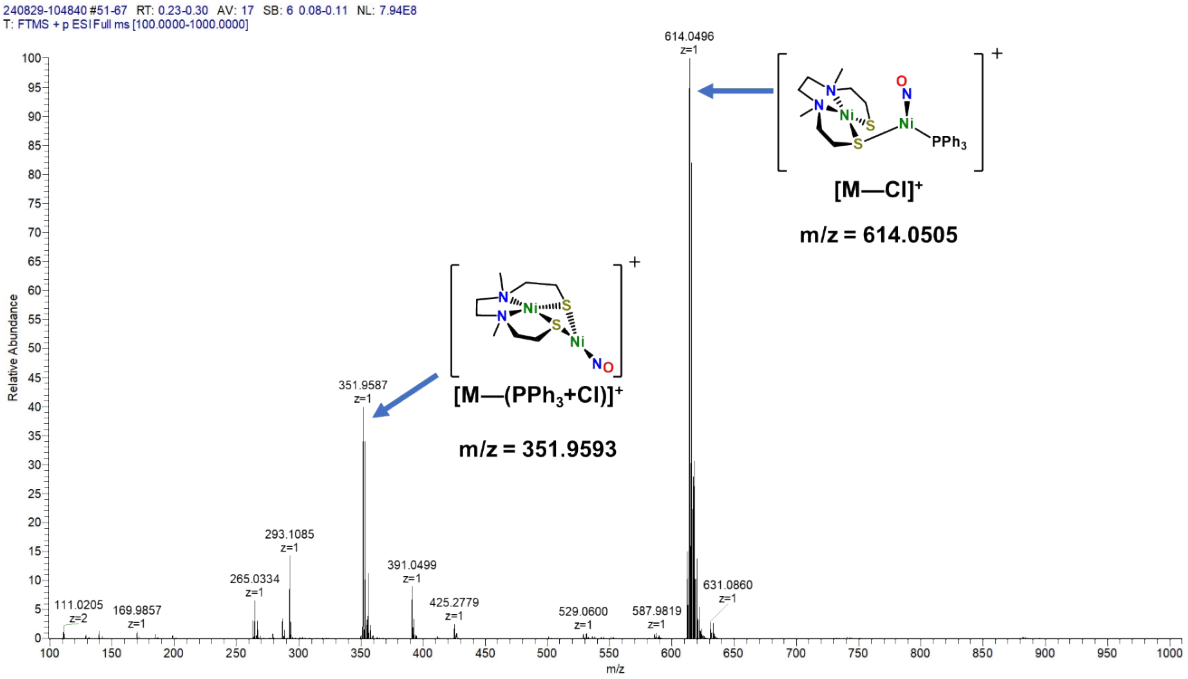

Figure S11. ESI-MS for [(bme-dame)Ni•Ni(NO)(Cl)(PPh_3)] complex in MeOH. The peak at m/z = 614.0496 corresponds to the $[(M+PPh_3)-(Cl)]^+$ species. The peak at m/z = 351.9587 corresponds to $[M—Cl]^+$ species.

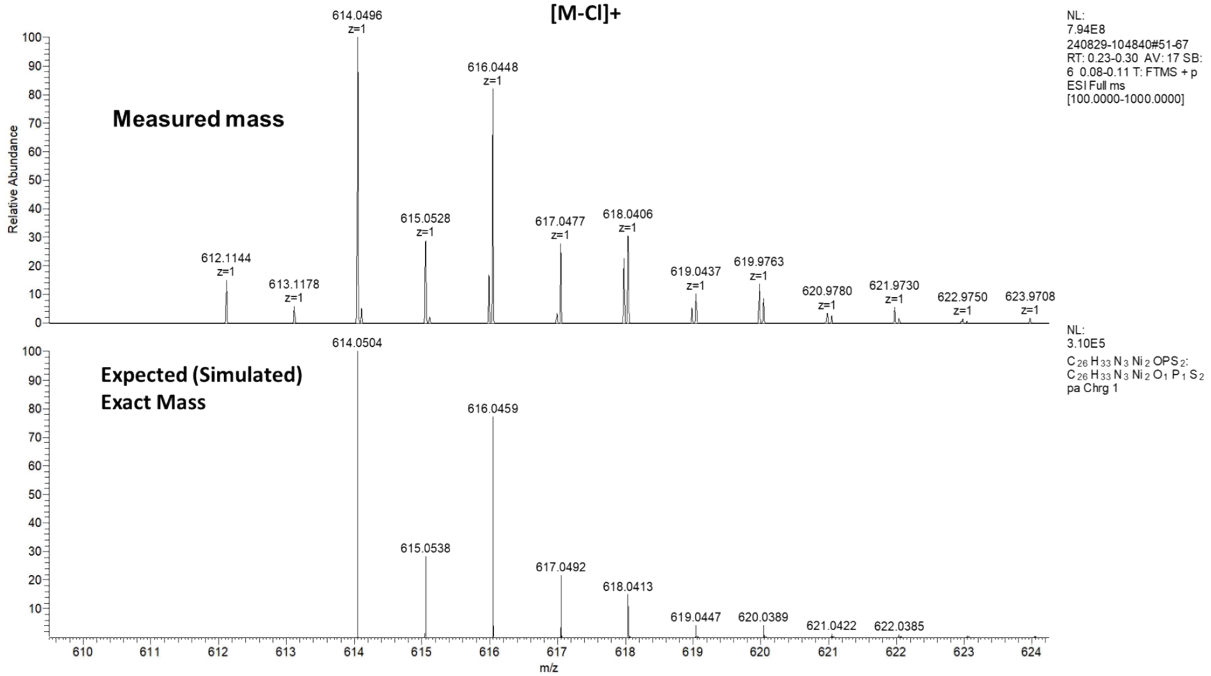

Figure S12. Experimental and simulated mass spectrum at m/z = 614.0496.

Table S2. Selected metric parameters for (dadt^{Bz})Ni,[16] Ni(NO)(Cl)(PPh_3)$_2$,[12] Ni(NO)(N_3)(PPh_3)$_2$,[18] complex 1 and complex 2 (CP2).

	Ni(dadt^{Bz})	Ni(NO)(Cl)(PPh_3)$_2$	Ni(NO)(N_3)(PPh_3)$_2$	Complex **1**	Complex **2**
∠Ni2-N3-O1 (°)	---	152.17	152.17	175.40	161.22
∠S1-Ni1-S2 (°)	84.11	---	---	82.17	83.87
∠N1-Ni1-N2 (°)	97.67	---	---	100.97	99.30
∠S1-Ni2-S2 (°)	---	---	---	76.64	107.64
∠Ni1-S1-Ni2 (°)	---	---	---	76.10	102.75
∠X-Ni2-N3 (°)	---	127.76	128.93	120.88	131.13
∠P1-Ni2-P2 (°)		120.67	120.13	---	---
Ni2-Cl1 (Å)	---	2.278	---	2.317	---
Ni2-N3 (Å)	---	1.681	1.690	1.646	1.658
Ni2-N4 (Å)	---	---	2.077	---	2.024
N3-O1 (Å)	---	1.160	1.170	1.158	1.179
Ni1-Ni2 (Å)	---	---	---	2.778	3.508
Ni-N_2S_2 (disp) (Å)	0.007	---	---	0.018	0.015 (N2S Plane)
Ni1-S (Å)	2.169,2.174	---	---	2.187, 2.190	2.160, 2.172
Ni2-S (Å)	---	---	---	2.317, 2.347	2.319, 2.327
τ_4 (Ni1)	0.10	---	---	0.13	0.18
τ_4 (Ni2)	---	0.79	0.79	0.83	0.84

Table S3. Crystal data and structure refinement for Ni_dame_Ni_NO_Cl_0m.

Identification code	Ni_dame_Ni_NO_Cl_0m
CCDC Number	**2380703**
Empirical formula	$C_{26}H_{33}ClN_3Ni_2OPS_2$
Formula weight	651.51
Temperature/K	110.0
Crystal system	triclinic
Space group	P-1
a/Å	9.7816(4)
b/Å	15.5698(6)
c/Å	18.7752(7)
α/°	92.798(2)
β/°	93.041(2)
γ/°	92.763(2)
Volume/Å^3	2848.29(19)
Z	4
ρ_{calc}g/cm^3	1.519

μ/mm^{-1}	4.601
F(000)	1352.0
Crystal size/mm^3	0.5 × 0.3 × 0.3
Radiation	CuKα (λ = 1.54178)
2Θ range for data collection/°	4.72 to 133.744
Index ranges	-11 ≤ h ≤ 11, -18 ≤ k ≤ 18, -22 ≤ l ≤ 22
Reflections collected	90413
Independent reflections	10058 [R_{int} = 0.0855, R_{sigma} = 0.0594]
Data/restraints/parameters	10058/4/651
Goodness-of-fit on F^2	1.090
Final R indexes [I>=2σ (I)]	R_1 = 0.0677, wR_2 = 0.1501
Final R indexes [all data]	R_1 = 0.0815, wR_2 = 0.1573
Largest diff. peak/hole / e Å^{-3}	1.54/-1.34

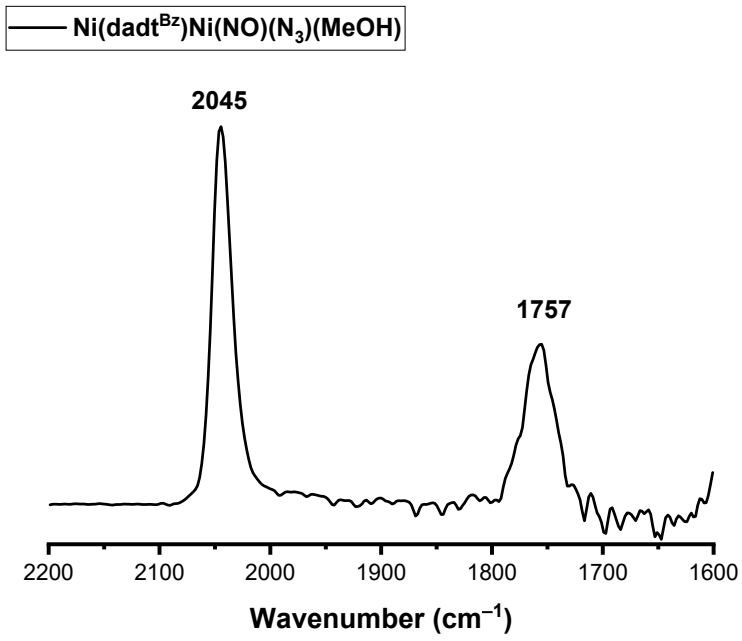

Figure S13. Solution (in MeOH) IR spectra of complex 2 showing ν(NO) and ν(N_3) stretching at 1757 cm^{-1} and 2045 cm^{-1} respectively.

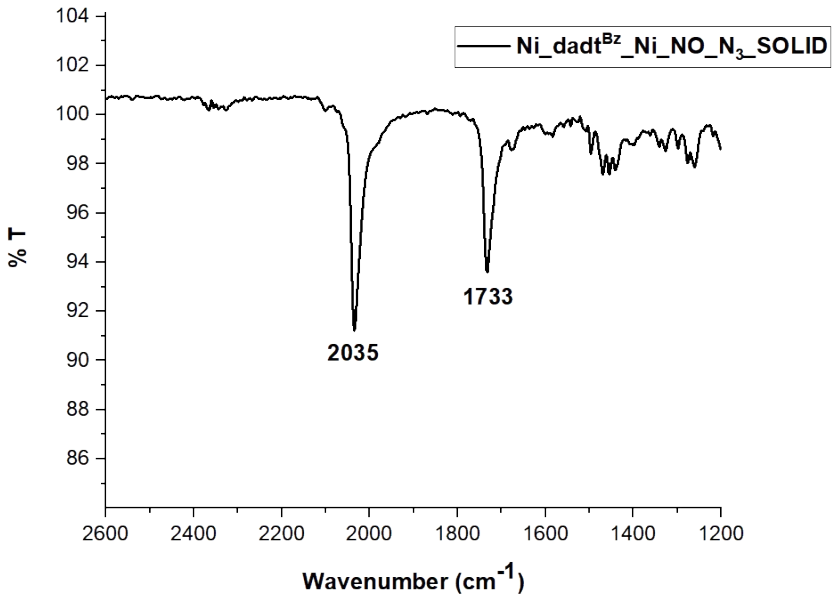

Figure S14. Solid IR spectra of complex 2 showing v(NO) and v(N_3) stretching at 1733 and 2035 cm^{-1} respectively.

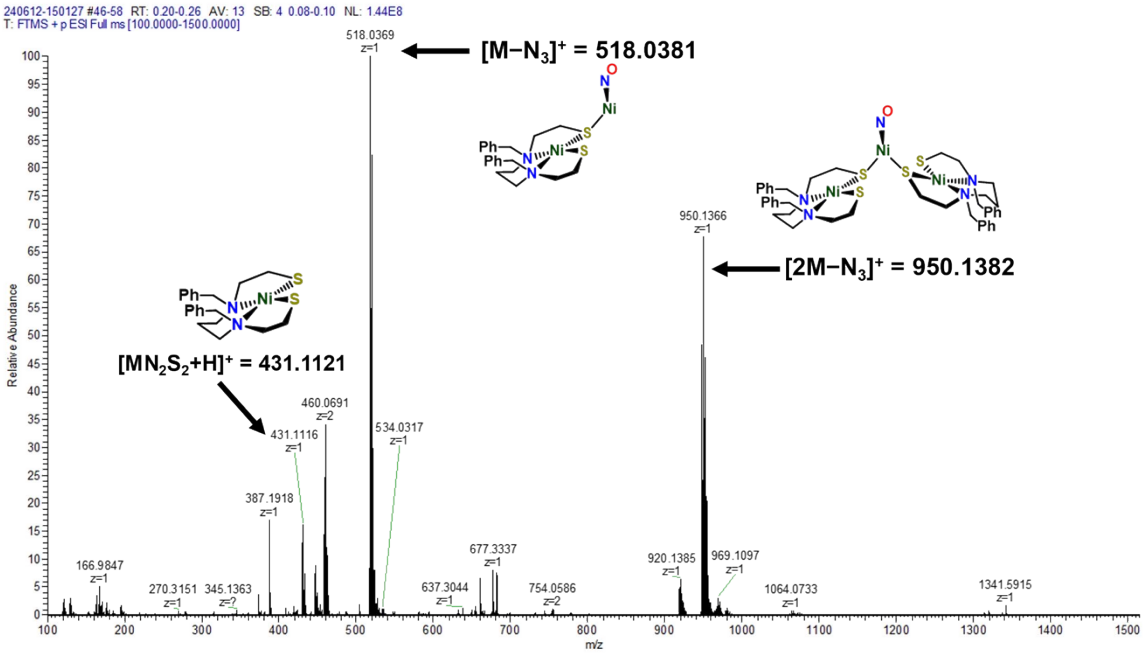

Figure S15. ESI-MS spectrum for complex 2 in MeOH/DMF mixture. The peak at m/z = 950.1366 corresponds to the $[2M-(N_3)]^+$ species. The peak at m/z = 518.0369 corresponds to $[M—N_3]^+$ species.

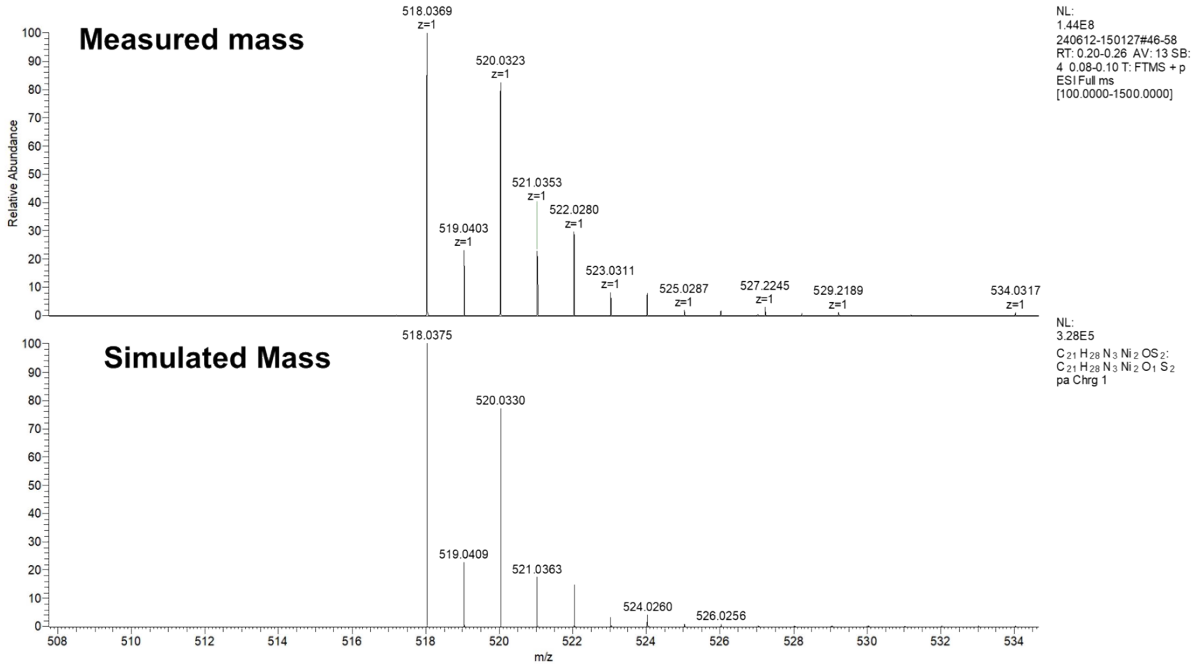

Figure S16. Experimental and simulated mass spectrum at m/z = 518.0375.

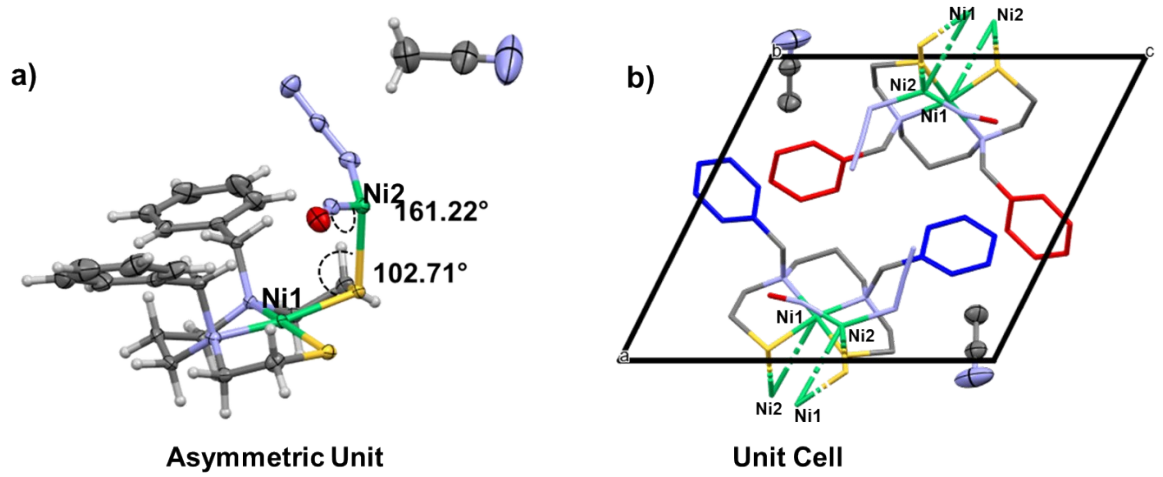

Figure S17. (a) Asymmetric unit of Complex **2** crystallized from MeCN/Ether (b) Unit cell of the molecule shows two asymmetric units and two MeCN molecules (as solvent of crystallization).

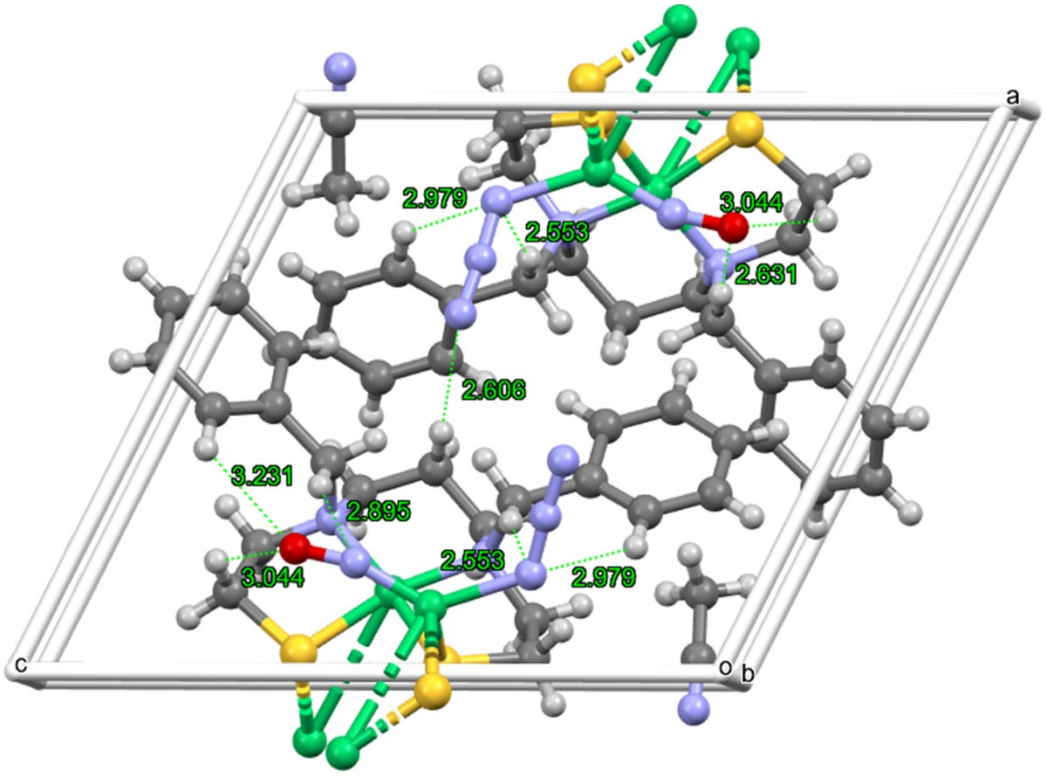

Figure S18. Short distances between the nitrosyl and azide groups to the nearby hydrogen atoms present in the unit cell of complex 2 crystalized from MeCN/Et_2O.

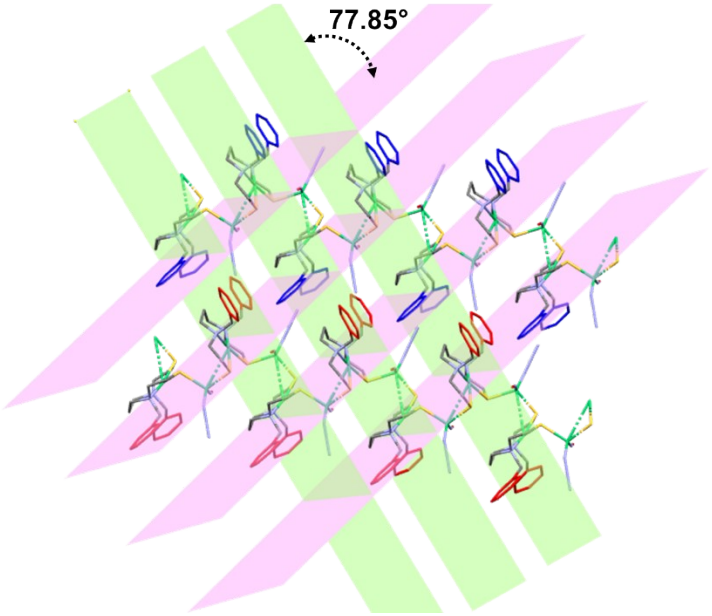

Figure S19. Angle between the planes created by benzene rings, the green planes are for the red benzene rings of layer 2 and the purple planes are for the blue benzene rings of layer 1.

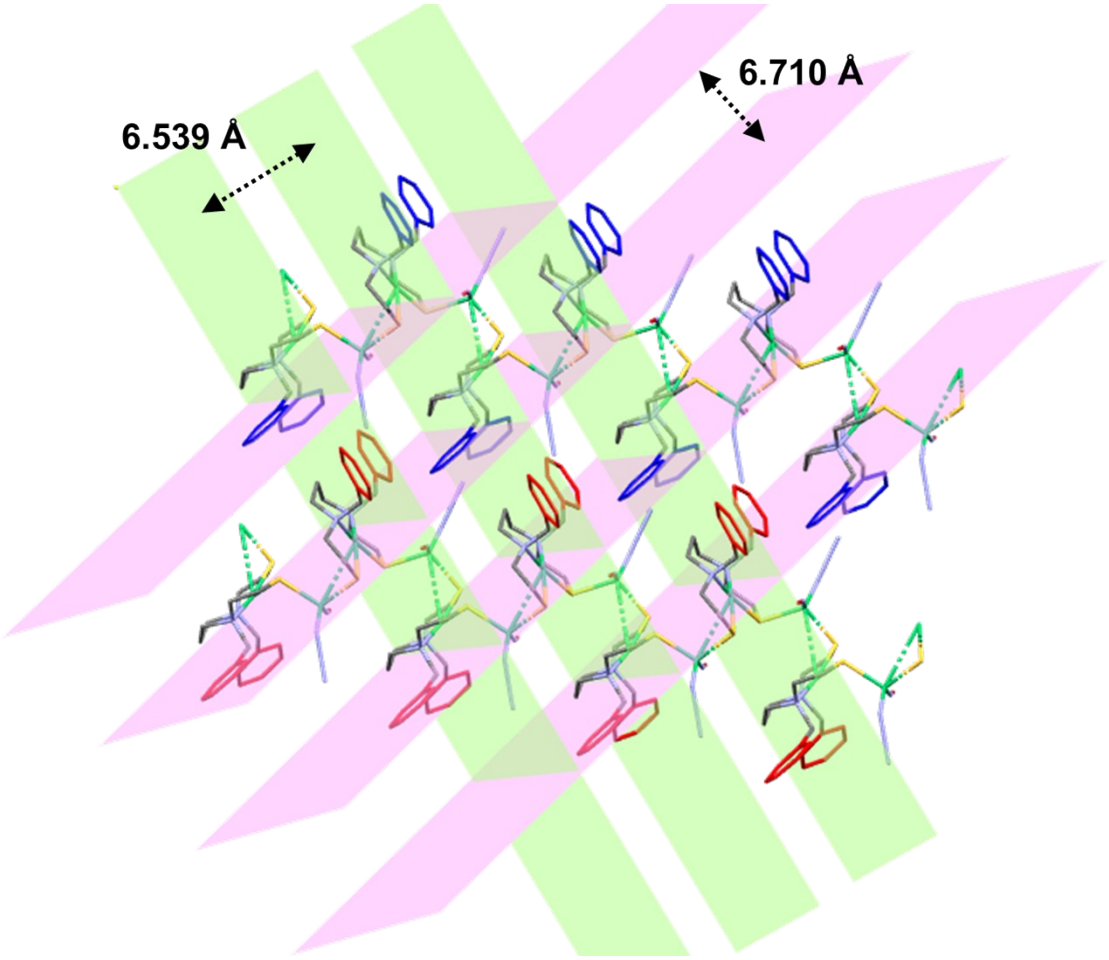

Figure S20. Distances between the planes created by benzene rings, the green planes are for the red benzene rings of layer 2 and the purple planes are for the blue benzene rings of layer 1.

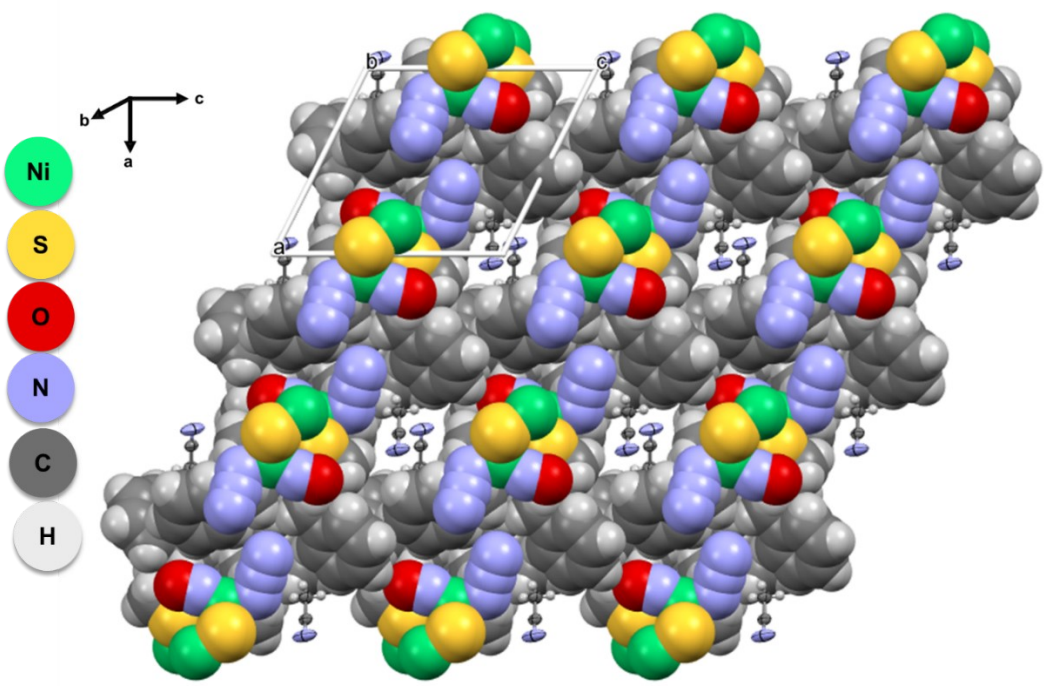

Figure S21. Crystal packing diagram of complex 2 ($MeCN/Et_2O$) in spacefill model viewed along b-axis shows the presence of CH_3CN molecules inside the cavity created by multiple layers of the coordination polymer.

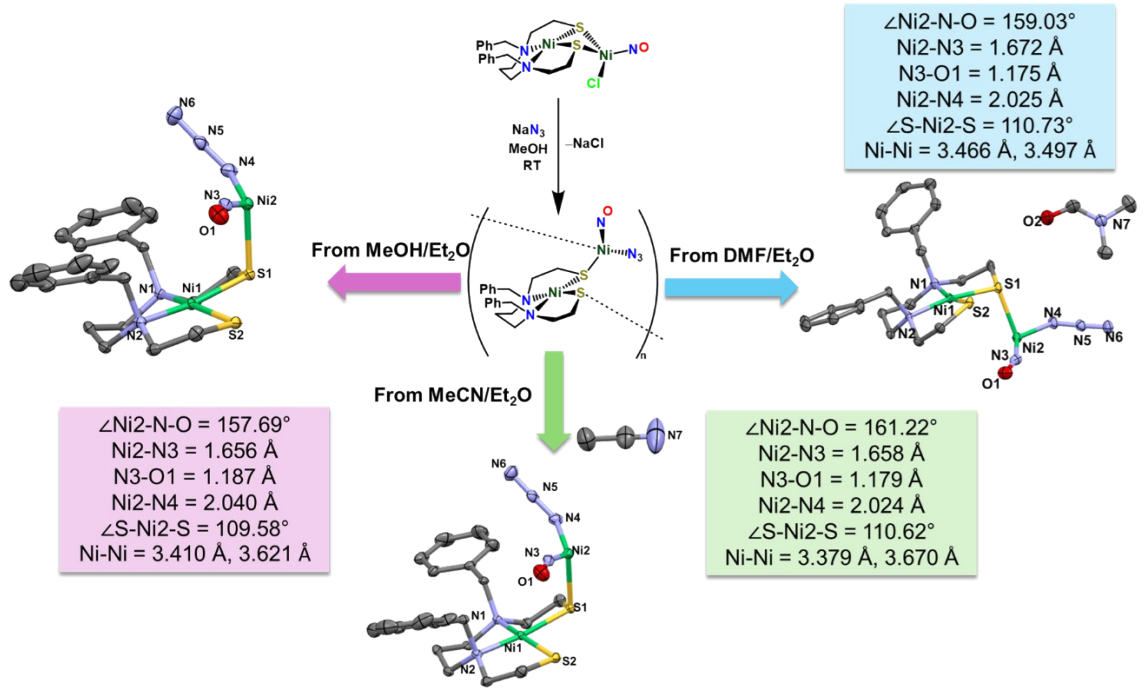

Figure S22. Synthesis of complex 2 and its crystallization in different solvents.

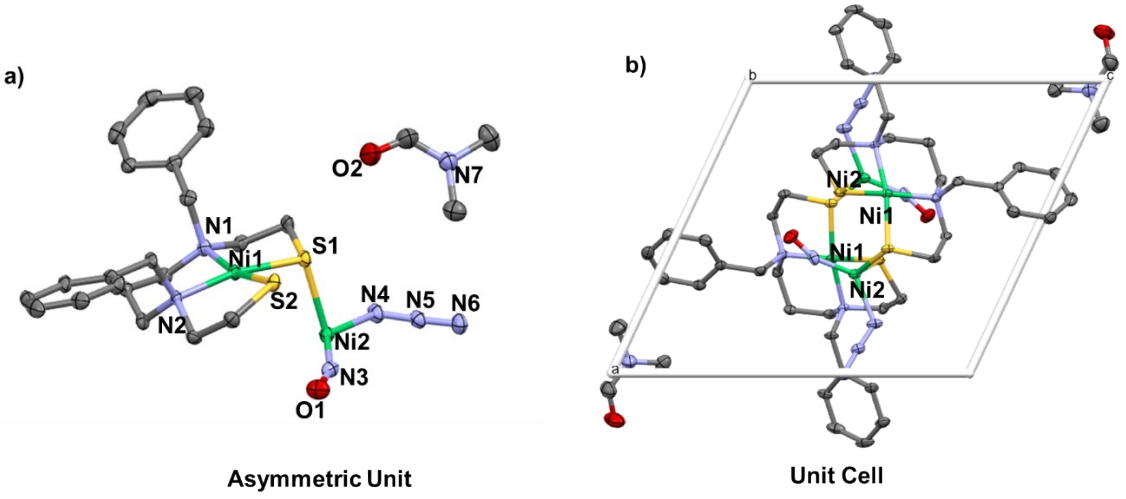

Figure S23. (a) Asymmetric unit of complex 2 crystallized from DMF/Ether (b) Unit cell of the molecule shows two asymmetric units and two DMF molecules as solvent of crystallization.

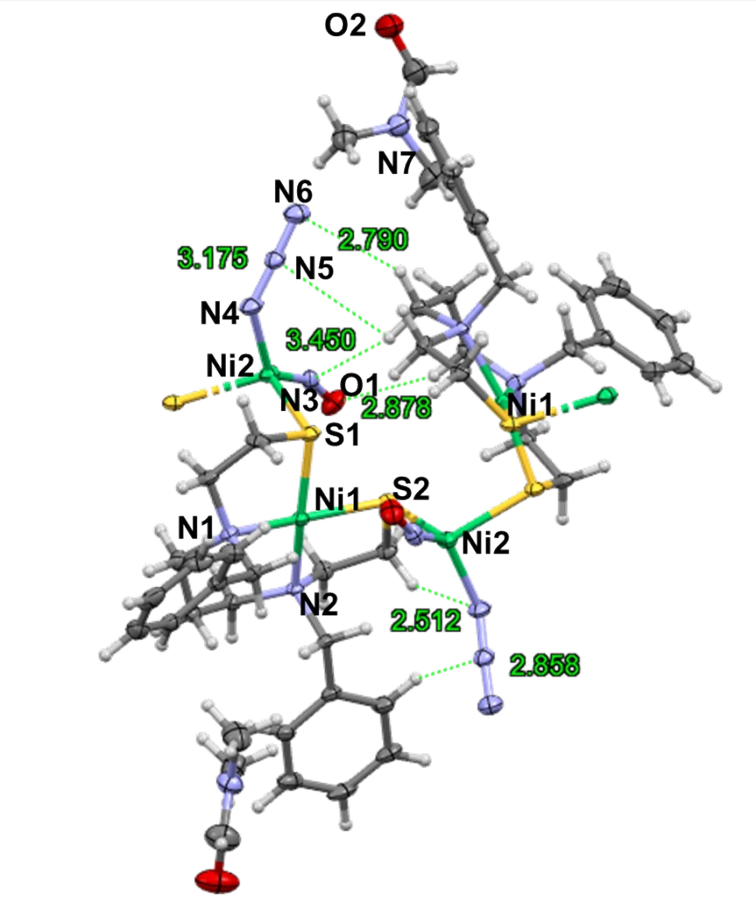

Figure S24. Short distances between the nitrosyl and azide groups to the nearby hydrogen atoms present in the unit cell of complex 2 crystalized from DMF/Et_2O.

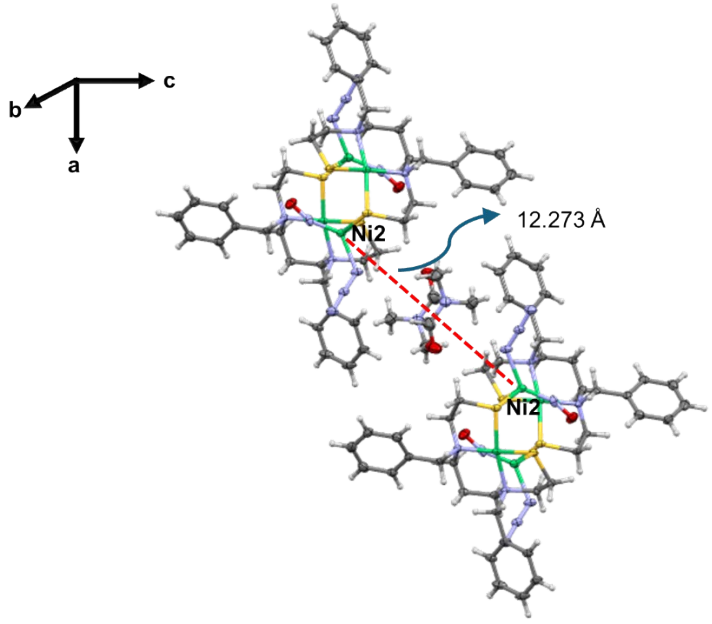

Figure S25. Crystal structure of complex 2 obtained from DMF/Et_2O showing the distance between the Ni centers (Ni2) in two adjacent layers (viewed along b-axis).

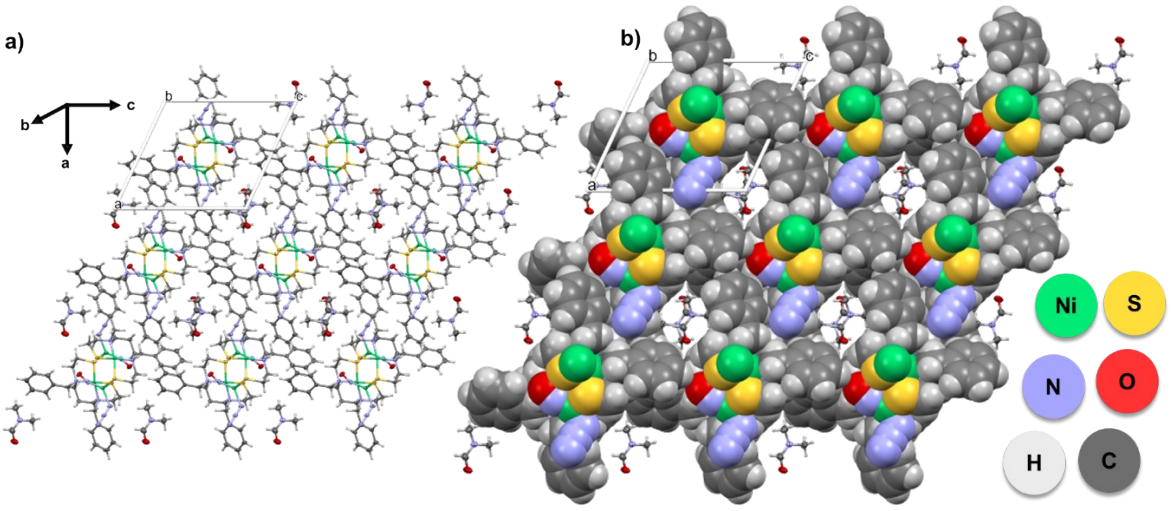

Figure S26. Crystal packing diagram of complex 2 (DMF/Et_2O) as (a) ellipsoid and (b) spacefill model viewed along b-axis shows the presence of DMF molecules inside the cavity created by multiple layers of the coordination polymer.

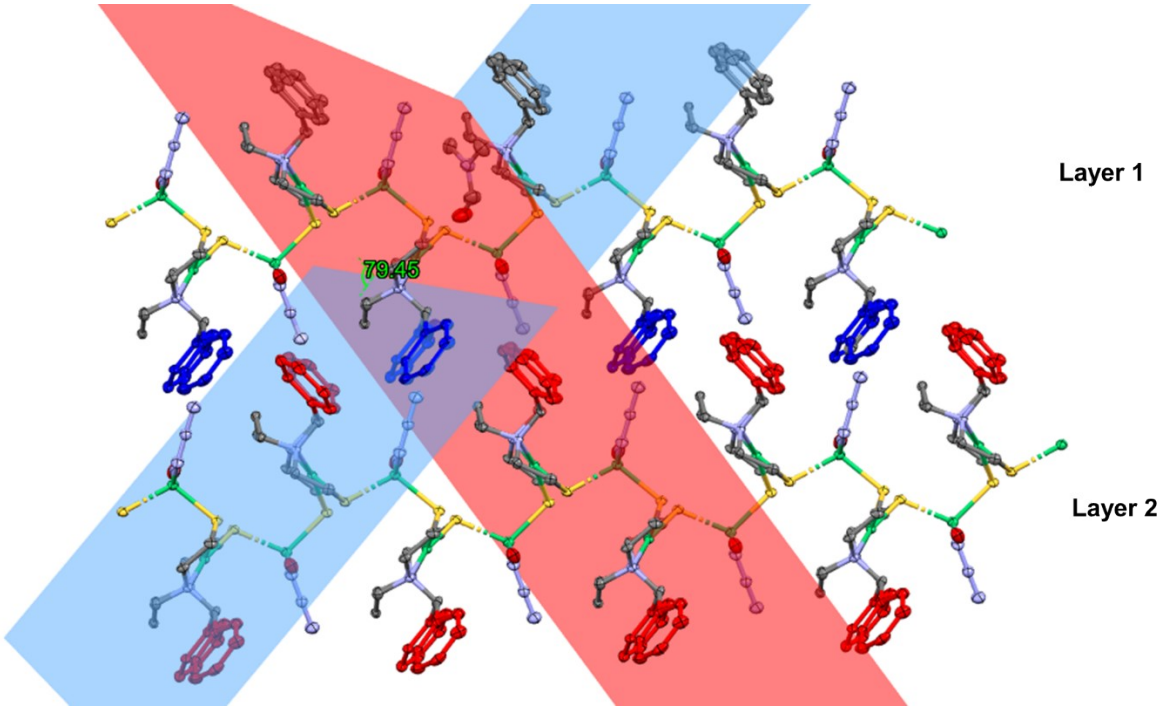

Figure S27. Angle between the planes created by benzene rings (79.45°) of complex 2 (DMF/Et_2O), the red plane is for red benzene ring of layer 2 and the blue plane is for the blue benzene ring of layer 1.

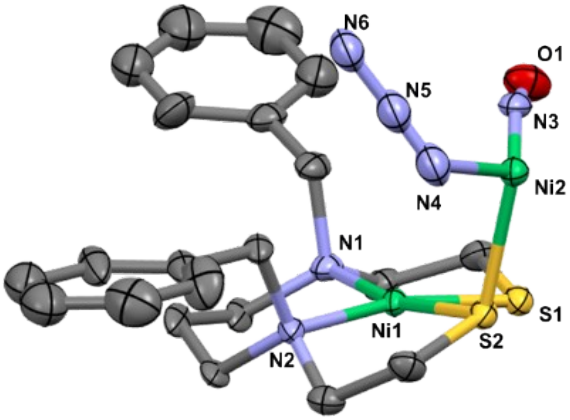

Figure S28. Single crystal x-ray structure for complex 2 crystallized from MeOH/Et_2O. Only asymmetric unit is shown.

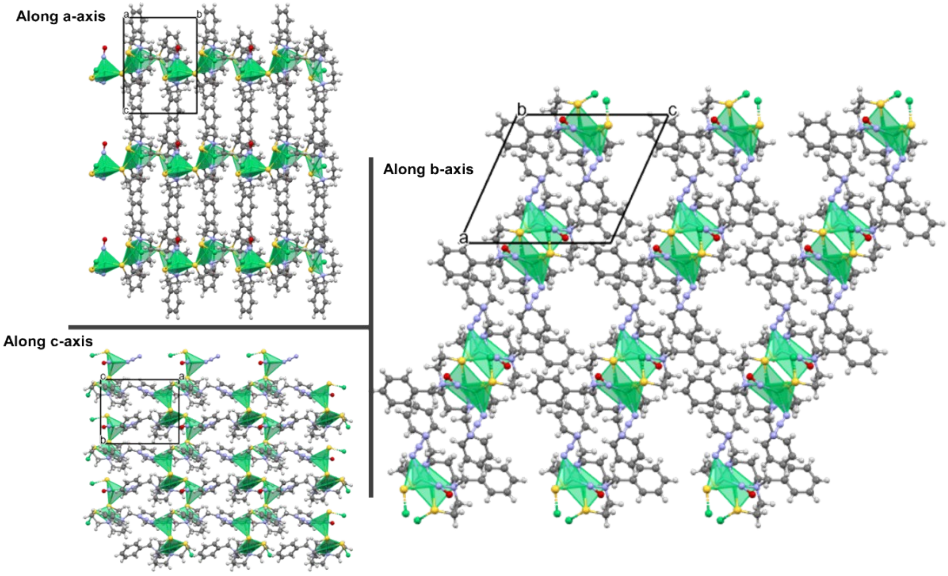

Figure S29. Crystal packing diagram of complex 2 along three crystallographic axes. The green polyhedral represents nickel centers.

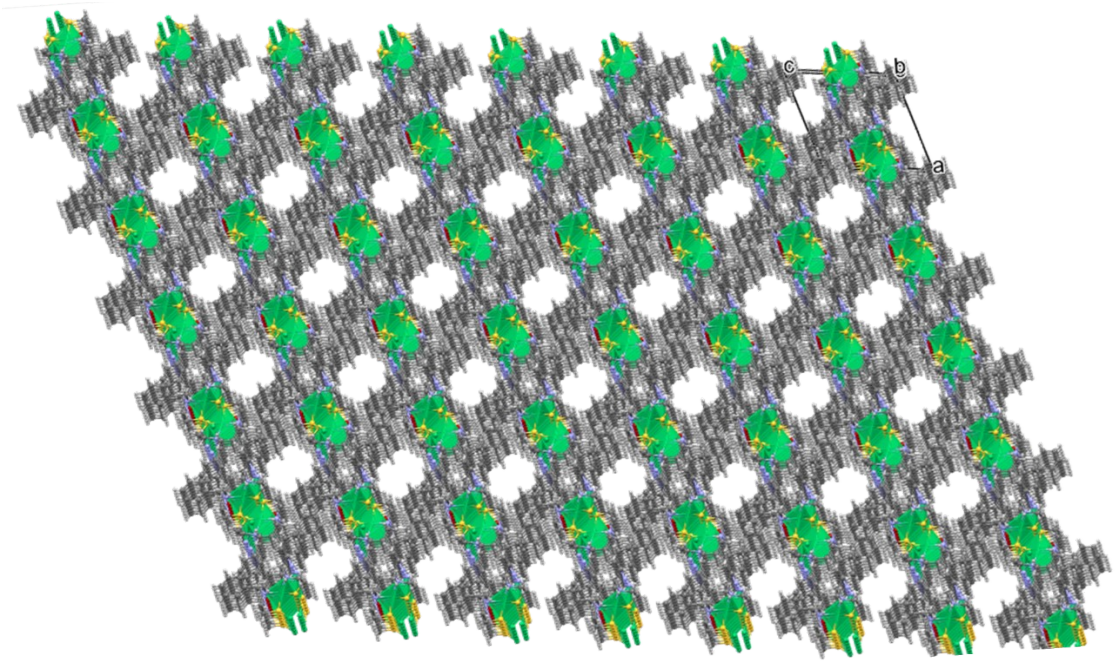

Figure S30. Crystal packing diagram of complex 2 (crystallized from MeOH/Ether) shows voids in the crystal lattice when viewed along b-axis.

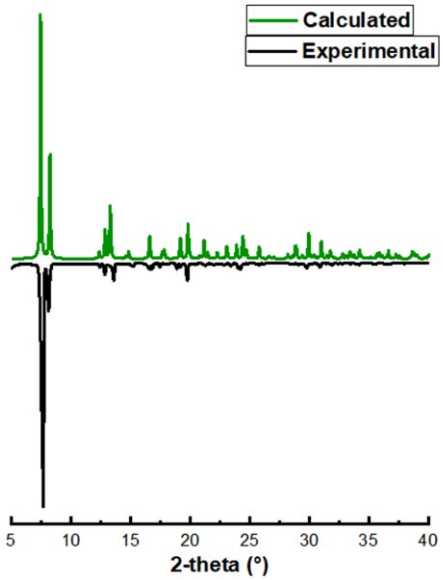

Figure S31. Experimental (black) and calculated (green) PXRD pattern for Complex **2**.

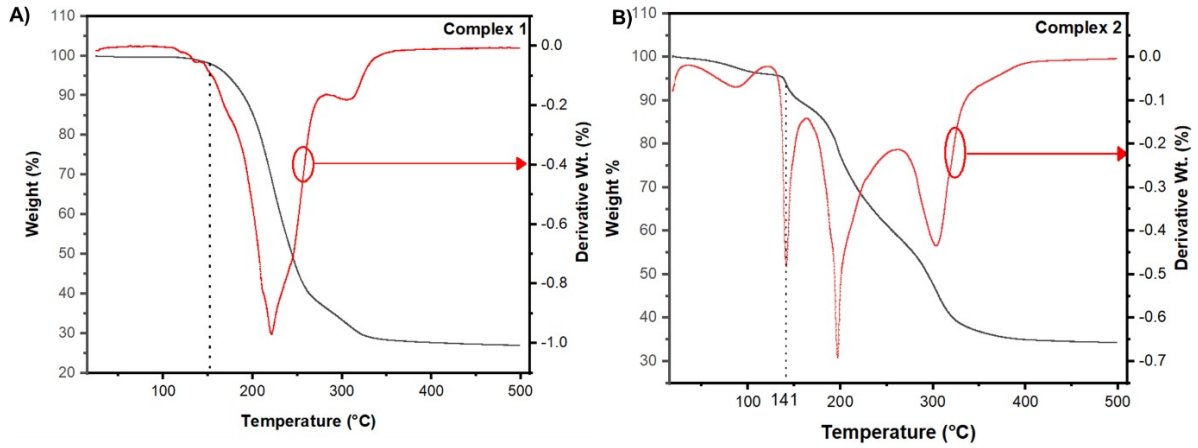

Figure S32. TGA data for complexes 1 and 2 under N_2.

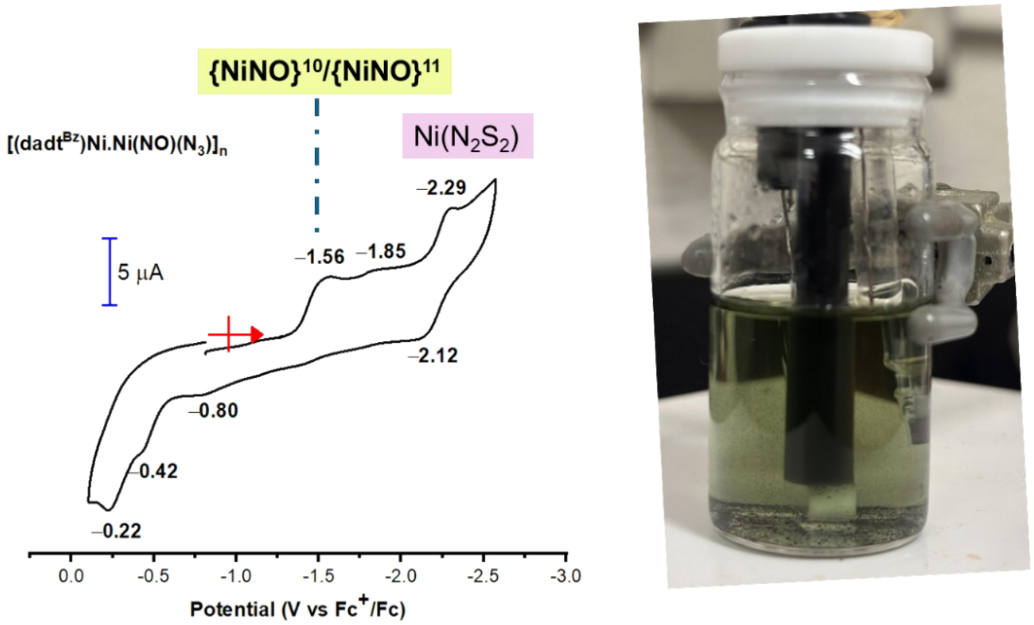

Figure S33. Cyclic voltammetry of complex 2 in DMF containing a 0.1 M [^{n}Bu$_4$N][PF$_6$] electrolyte and 2.0 mM complex at room temperature. The picture on the right shows very poor solubility of the coordination polymer in DMF even after stirring overnight.

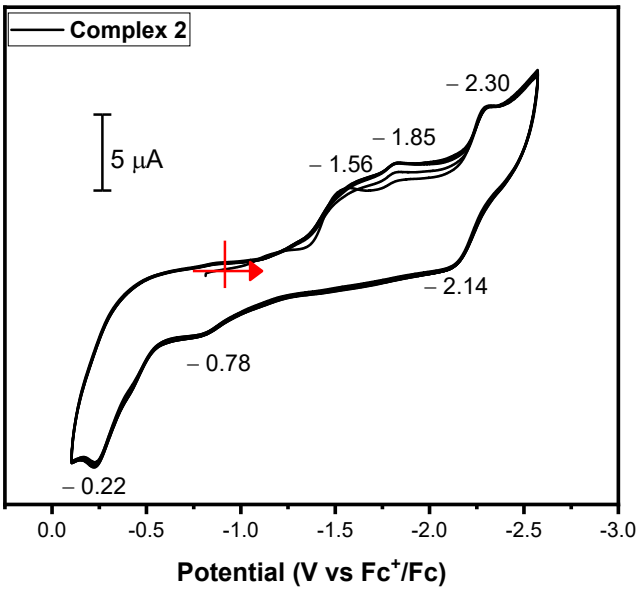

Figure S34. Cyclic voltammetry of complex 2 in DMF (multiple scans, no of scans = 6) containing a 0.1 M [$^{n}Bu_4N$][PF_6] electrolyte and 2.0 mM complex at room temperature. Low current intensity is attributed to the poor solubility of complex 2.

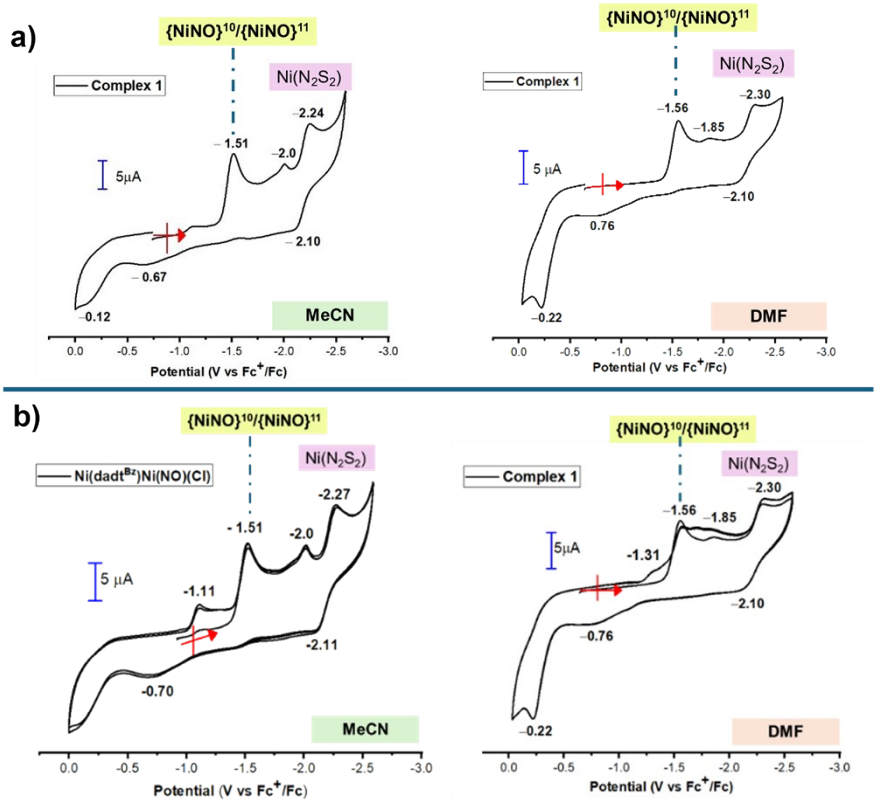

Figure S35. Cyclic voltammetry of complex **1** in MeCN (left) and DMF (right) containing a 0.1 M [$^{n}Bu_4N$][PF_6] electrolyte and 2.0 mM analyte at room temperature. Glassy carbon was used as the working electrode, platinum wire as the counter electrode, and Ag^0/AgCl as the reference electrode. All potentials were referenced to the Fc/Fc^+ couple at 0.00 V. B) Multiple scans (6 scans) for Complex **1** in MeCN and DMF.

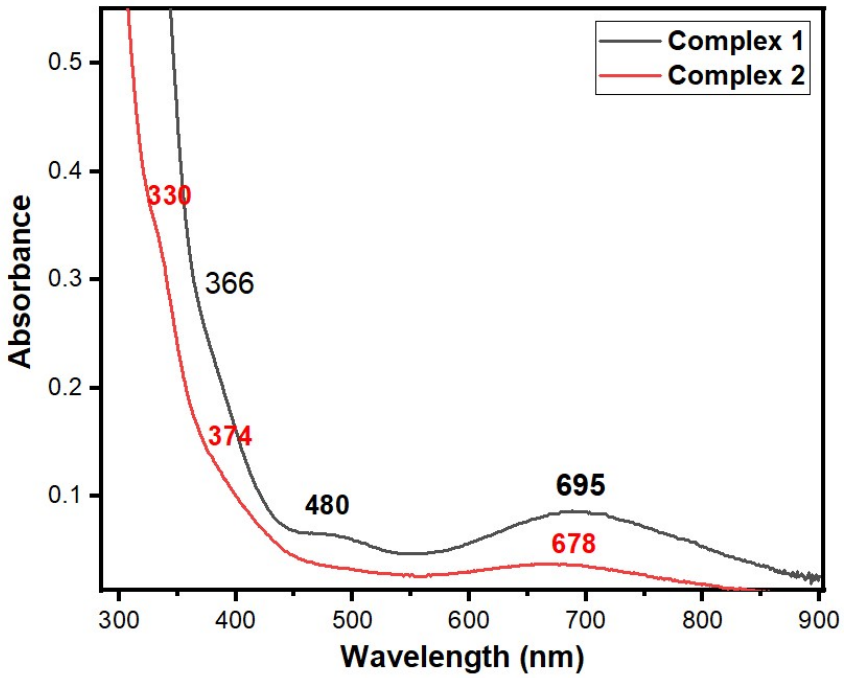

Figure S36. UV-vis spectrum for Complexes **1** and **2** in DMF. Note that the coordination polymer, Complex 2 is only sparingly soluble in DMF.

Hirshfeld Surface Analysis:

In order to evaluate intermolecular interactions present in the crystal lattice we have performed Hirshfeld surface analysis on crystal structures for complexes 1 and 2 (obtained from different solvents) using CrystalExplorer 21.5 software.[35] The Hirshfeld surface is mapped in 3D d_{norm} ($d_{|e|}$ + $d_{|i|}$) where d_e is the shortest distance between the Hirshfeld surface and atoms outside the molecular surface and d_i is the corresponding shortest distance to the nearest atoms inside the surface. On the Hirshfeld surface (d_{norm}) the red spots indicate the short interactions present in the molecule.

The quantitative measures of the Hirshfeld surface for complex 1 are total volume (566.55 Å^3), area (438.93 Å^3), globularity (0.754), and asphericity (0.110). The value of globularity $<$ 1.0 indicates a more structured molecular surface. The structural anisotropy of the compound is given by asphericity value. The Hirshfeld surface for complex 1 is shown in Figure S37, where the major interactions are found to be H···H (~50%), C···H (~14%) and O···H (~10%) respectively. The pie-chart presented in Figure S37e shows different types of interactions in complex 1.

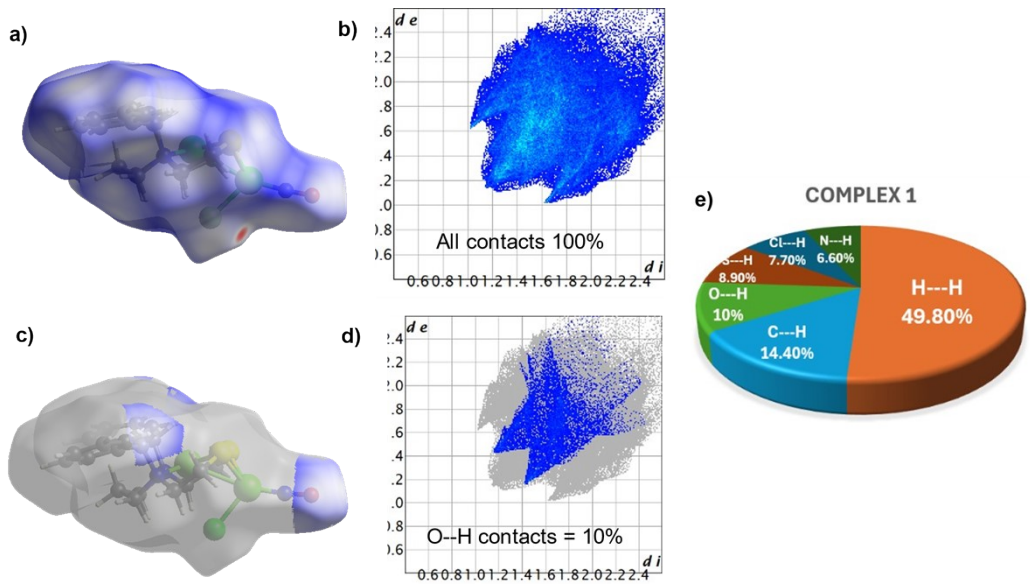

Figure S37. a) Hirshfeld surface mapped in 3D d_{norm}. The red area shows strong interactions (shorter than van der Waals contacts), while blue (longer than van der Waals contacts) and white (van der Waals contacts) correspond to weak interactions. (b) All interactions shown by 2D fingerprint for complex **1**. (c) Hirshfeld surface mapped for O—H contacts and (d) the corresponding 2D fingerprint region. (e) The pie-chart shows percentage of different kinds of interactions present in complex 1.

For complex 2 (crystalized from MeCN/Et_2O), the quantitative measures of the Hirshfeld surface are total volume (569.86 Å^3), area (439.16 Å^3), globularity (0.757), and asphericity (0.104). The Hirshfeld surface analysis suggests that the majority of interactions are between the H—H (43%). The next major interaction is due to the N—H contacts (24%), which accounts for hydrogen bonding interaction between the azide group and the aromatic as well as aliphatic hydrogens as shown in Figure 38c with red arrows. The O—H contacts between the oxygen atom of the nitrosyl group and the aromatic and aliphatic hydrogens are also observed from the Hirshfeld surface analysis, as indicated in figure 38d, with red arrows.

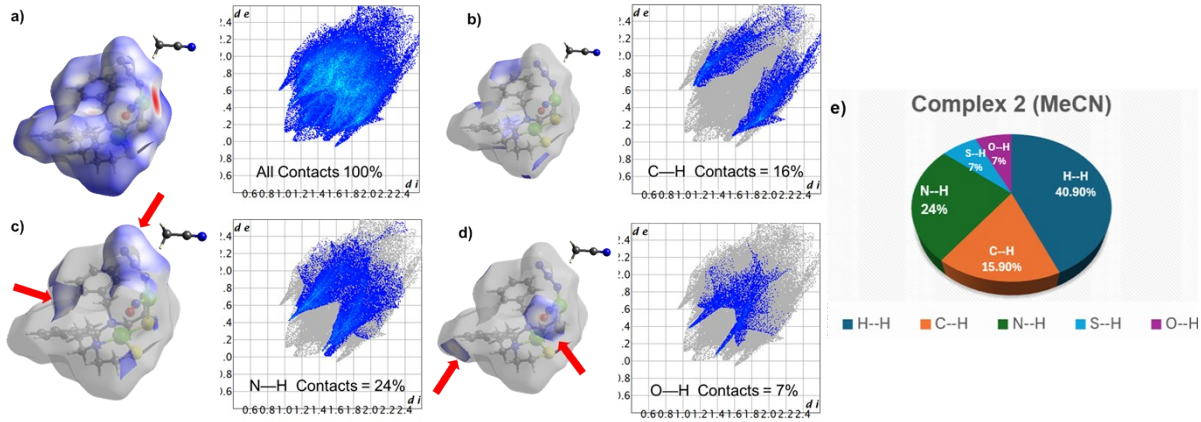

Figure S38. (a) Hirshfeld surface mapped in 3D d_{norm}. The major interactions shown by 2D fingerprint for complex 2 (MeCN). (b) Hirshfeld surface mapped for C—H contacts and the corresponding 2D fingerprint region. (c) Hirshfeld surface mapped for N—H contacts and the corresponding 2D fingerprint region. (d) Hirshfeld surface mapped for O—H contacts and the corresponding 2D fingerprint region. The red arrows indicate the positions where the intermolecular interactions occur. (e) The pie-chart shows percentage of different kinds of interactions present in complex 2 (MeCN).

In case of complex 2 (crystalized from DMF/Et_2O), the quantitative measures of the Hirshfeld surface are total volume (553.37 Å^3), area (455.55 Å^3), globularity (0.716), and asphericity (0.125). The Hirshfeld surface analysis suggests that the majority of interactions are between the H—H (42%). The next major interaction is due to the N—H contacts (24%), which accounts for hydrogen bonding interaction between the azide group and the aromatic as well as aliphatic hydrogens as shown in Figure S39c with green arrows. C—H contacts account for 14% of the interactions, which are mainly due to the CH—π interaction. The O—H contacts between the oxygen atom of the nitrosyl group and the aromatic protons are also observed in the Hirshfeld surface analysis, as indicated in Figure S39d, with green arrows.

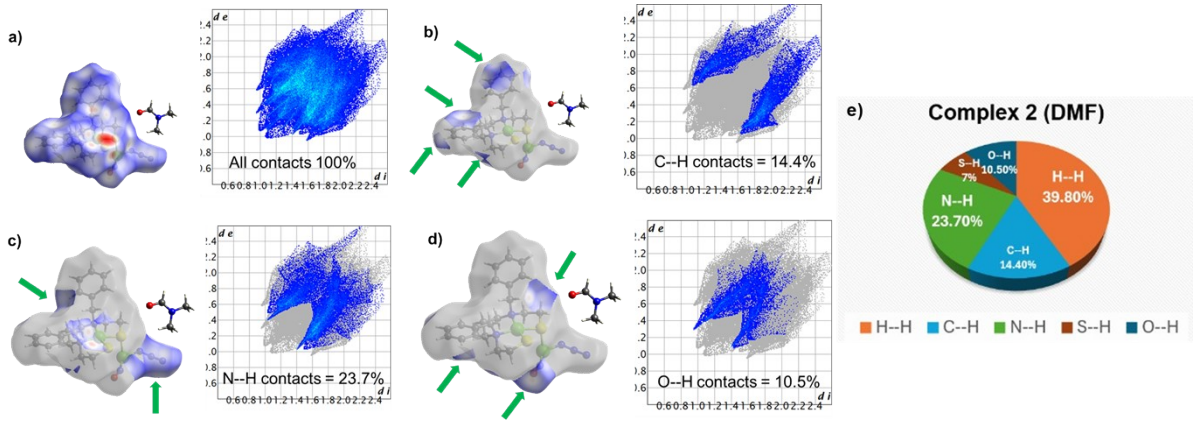

Figure S39. (a) Hirshfeld surface mapped in 3D d_{norm}. All interactions shown by 2D fingerprint for complex **2** (DMF). (b) Hirshfeld surface mapped for C—H contacts and the corresponding 2D fingerprint region. (c) Hirshfeld surface mapped for N—H contacts and the corresponding 2D fingerprint region. (d) Hirshfeld surface mapped for O—H contacts and the corresponding 2D fingerprint region. The green arrows indicate the positions where the intermolecular interactions occur. (e) The pie-chart shows percentage of different kinds of interactions present in complex 2 (DMF).

The quantitative measures of the Hirshfeld surface for complex 2 when crystalized from MeOH are total volume (635.67 Å^3), area (483.37 Å^3), globularity (0.740), and asphericity (0.102). The Hirshfeld surface analysis suggests that the majority of interactions are between the H—H (47%). The next major interaction is due to the N—H contacts (23%), which accounts for hydrogen bonding interaction between the azide group and the aromatic as well as aliphatic hydrogens as shown in Figure S40c with plum arrows. C—H contacts account for 12% of the interactions, which are mainly due to the CH—π interaction. The O—H contacts between the oxygen atom of the nitrosyl group and the aromatic protons are also observed in the Hirshfeld surface analysis, as indicated in Figure S40d, with plum arrows.

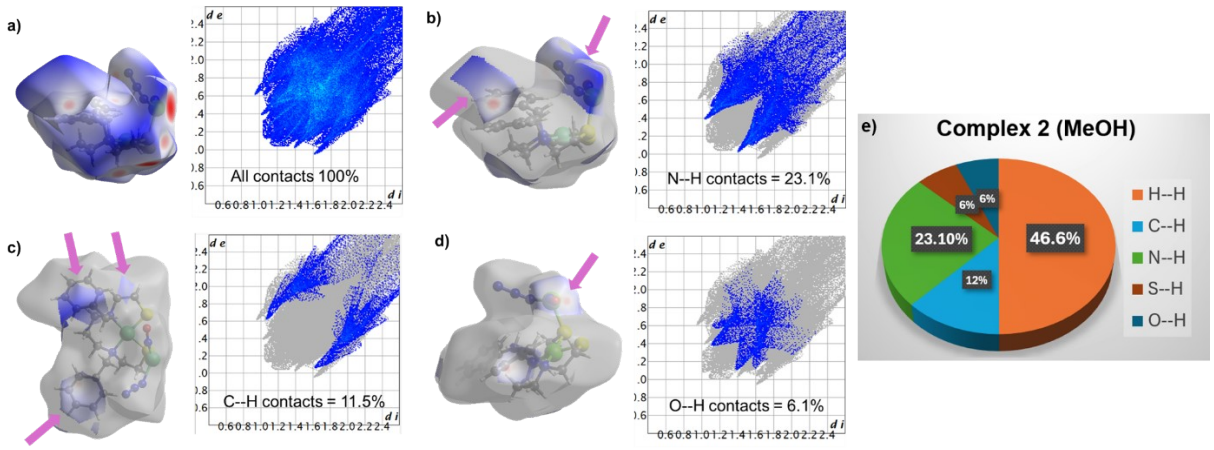

Figure S40. (a) Hirshfeld surface mapped in 3D d_{norm}. All interactions shown by 2D fingerprint for complex 2 (**MeOH**). (b) Hirshfeld surface mapped for N—H contacts and the corresponding 2D fingerprint region. (c) Hirshfeld surface mapped for C—H contacts and the corresponding 2D fingerprint region. (d) Hirshfeld surface mapped for O—H contacts and the corresponding 2D fingerprint region. The plum arrows indicate the positions where the intermolecular interactions occur. (e) The pie-chart shows percentage of different kinds of interactions present in complex 2 (MeOH).

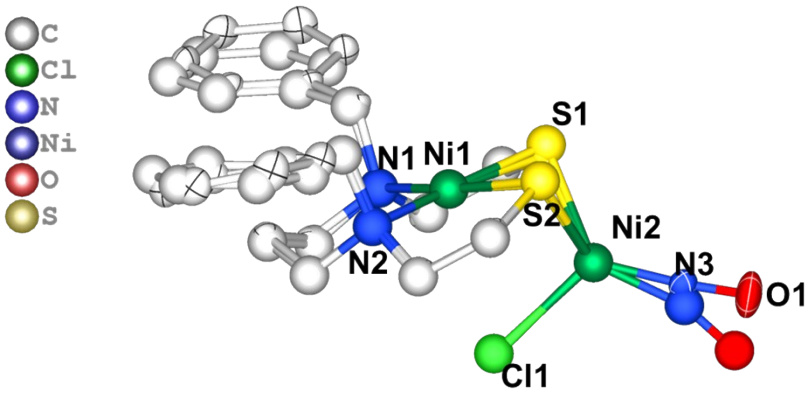

	Calculated	Experimental
Ni1-Ni2 (Å)	2.824	2.778
Ni2-N3 (Å)	1.749	1.646
N3-O1 (Å)	1.177	1.158
∠Ni2-N3-O1 (°)	163.16	175.40
Ni2-Cl1(Å)	2.378	2.317
Ni1disp (Å)	0.021	0.018
τ_4 (Ni1)	0.12	0.13
τ_4 (Ni2)	0.73	0.83
v (NO) (cm^{-1})	1761 (in MeOH)	1756 (in MeOH)

Figure S41. Superposition of the crystal structure and the optimized structure (in the broken symmetry state using the B3LYP functional[22]) of complex 1 . Hydrogen atoms are removed for clarity. The calculated and experimental bond distances and angles are given in the table.

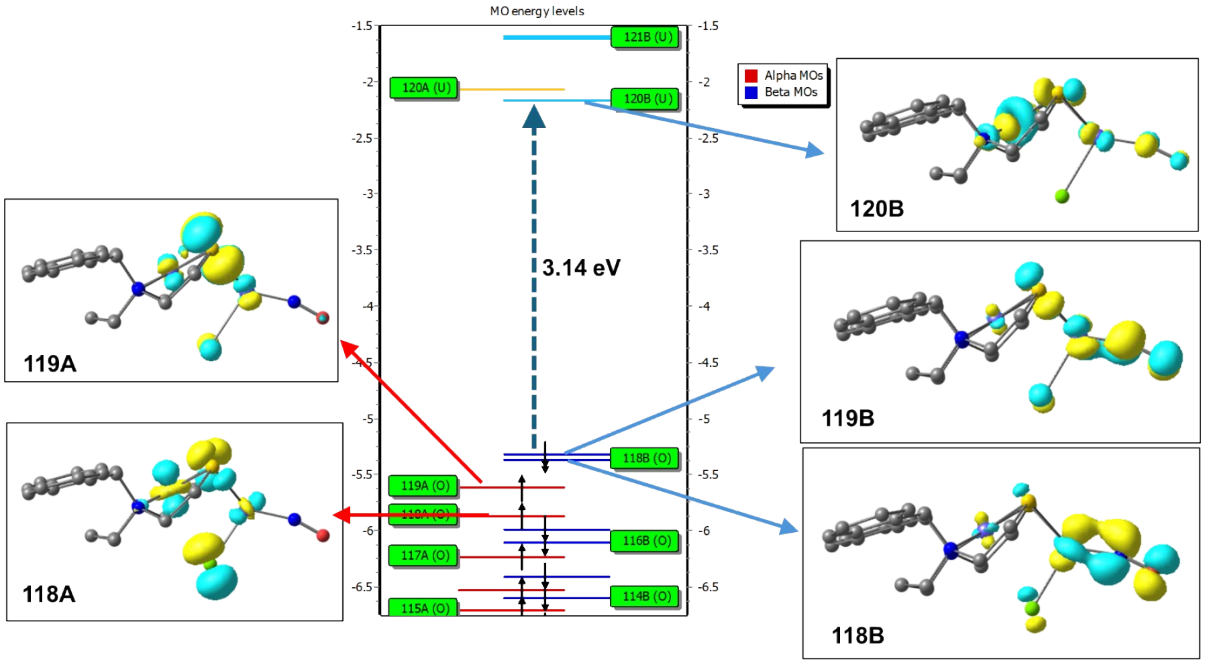

Figure S42. DFT optimized complex 1 as OSS in B3LYP functional showing the corresponding alpha and beta molecular orbitals (Contour Value = 0.06).

Table S4*. Calculated* metric parameters for complex 1 [Ni(dadt^{Bz})•Ni(NO)(Cl)] and hypothetical monomeric complex 2 [Ni(dadt^{Bz})•Ni(NO)(N$_3$)] as OSS in B3LYP[22] and as CSS in TPSS[21] functional.

	B3LYP		TPSS	
	Ni(N_2S_2)•Ni(NO)(Cl)	Ni(N_2S_2)•Ni(NO)(N_3)	Ni(N_2S_2)•Ni(NO)(Cl)	Ni(N_2S_2)•Ni(NO)(N_3)
	OSS	**OSS**	**CS**	**CS**
Ni2—N (Å)	1.75	1.75	1.66	1.67
N—O (Å)	1.17	1.18	1.18	1.18
Ni2—X (Å)	2.38	2.00	2.38	1.96
Ni1-X (Å)	3.02	2.77	2.93	2.71
Ni1—Ni2 (Å)	2.82	2.75	2.72	2.69
Ni2—S (Å)	2.49, 2.49	2.49, 2.49	2.41, 2.41	2.36, 2.53
Ni1—S (Å)	2.29	2.27	2.25	2.23, 2.24
∠Ni-N-O (°)	163.16	147	159	152.8
∠Ni1-S-Ni2 (°)	72.29	70.36, 70.34	71.24	68.33, 71.57
∠S1-Ni1-S2 (°)	83.67	83.34	82.89	82.69
∠S1-Ni2-S2 (°)	75.56	74.61	76.37	74.06
∠X-Ni2-NO (°)	111.48	106.66	130.38	121.72
Mulliken Charges (NO)	0.020,−0.183	−0.006, −0.186	0.062, −0.165	0.040, −0.180
τ_4 (Ni2)	0.73	0.69	0.81	0.76

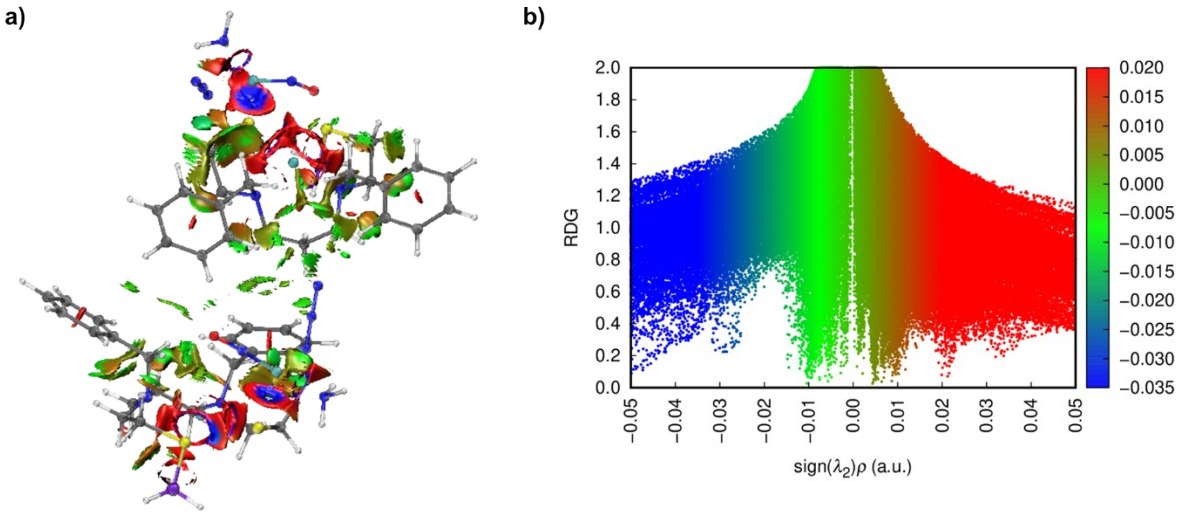

Figure S43. Visual analysis of intermolecular interactions between two asymmetric units of complex 2 (energy minimized structure in CSS B3LYP calculations in gas phase) obtained by DFT calculations and visualized by Multiwfn 3.8 (dev)[24,25] and VMD 1.9.3 programs.[26]

Table S5. Crystal data and structure refinement for MJ_Ni_Ni_Cl_PPh3_0m.

Identification code	Trimetallic Complex
CCDC Number	**2378998**
Empirical formula	$C_{46}H_{62}Cl_4N_6Ni_4S_4$
Formula weight	1203.89
Temperature/K	110.00
Crystal system	triclinic
Space group	P-1
a/Å	12.1770(10)
b/Å	12.5543(10)
c/Å	18.8033(15)
α/°	85.080(2)
β/°	82.619(3)
γ/°	63.925(2)
Volume/Å^3	2559.2(4)
Z	2
ρ_{calc}g/cm^3	1.562
μ/mm^{-1}	1.860
F(000)	1248.0
Crystal size/mm^3	0.5 × 0.5 × 0.3
Radiation	MoKα (λ = 0.71073)
2Θ range for data collection/°	4.162 to 51.122
Index ranges	-14 ≤ h ≤ 14, -15 ≤ k ≤ 15, -22 ≤ l ≤ 22
Reflections collected	54246
Independent reflections	9420 [R_{int} = 0.0573, R_{sigma} = 0.0398]
Data/restraints/parameters	9420/0/582
Goodness-of-fit on F^2	1.039
Final R indexes [I>=2σ (I)]	R_1 = 0.0322, wR_2 = 0.0826
Final R indexes [all data]	R_1 = 0.0439, wR_2 = 0.0886
Largest diff. peak/hole / e Å^{-3}	1.03/-0.48

Table S6. Crystal data and structure refinement for complex 1.

Identification code	complex 1
CCDC Number	**2195745**
Empirical formula	$C_{21}H_{28}ClN_3Ni_2OS_2$
Formula weight	555.45
Temperature/K	110.0
Crystal system	monoclinic
Space group	$P2_1/c$
a/Å	12.8828(7)
b/Å	24.2495(13)
c/Å	7.6958(4)
α/°	90
β/°	106.9590(10)
γ/°	90
Volume/Å^3	2299.6(2)
Z	4
ρ_{calc}g/cm^3	1.604
μ/mm^{-1}	4.945
F(000)	1152.0
Crystal size/mm^3	0.1 × 0.1 × 0.05
Radiation	CuKα (λ = 1.54178)
2Θ range for data collection/°	7.174 to 136.996
Index ranges	-15 ≤ h ≤ 15, -29 ≤ k ≤ 29, -8 ≤ l ≤ 9
Reflections collected	65673
Independent reflections	4235 [R_{int} = 0.0707, R_{sigma} = 0.0242]
Data/restraints/parameters	4235/0/271
Goodness-of-fit on F^2	1.124
Final R indexes [I>=2σ (I)]	R_1 = 0.0338, wR_2 = 0.0841
Final R indexes [all data]	R_1 = 0.0369, wR_2 = 0.0862
Largest diff. peak/hole / e Å^{-3}	0.29/-0.55

Table S7. Crystal data and structure refinement for complex 2 (obtained from MeCN/Et_2O).

Identification code	complex 2 (MeCN/Et_2O)
CCDC Number	**2368992**
Empirical formula	$C_{23}H_{31}N_7Ni_2OS_2$
Formula weight	603.09
Temperature/K	110.0
Crystal system	monoclinic
Space group	$P2_1$
a/Å	12.1727(4)
b/Å	8.9902(3)
c/Å	13.4302(6)
α/°	90
β/°	116.6370(10)
γ/°	90
Volume/Å^3	1313.74(9)
Z	2
ρ_{calc}g/cm^3	1.525
μ/mm^{-1}	3.511
F(000)	628.0
Crystal size/mm^3	0.5 × 0.5 × 0.3
Radiation	CuKα (λ = 1.54178)
2Θ range for data collection/°	8.126 to 140.528
Index ranges	-14 ≤ h ≤ 14, -10 ≤ k ≤ 10, -16 ≤ l ≤ 16
Reflections collected	28082
Independent reflections	5020 [R_{int} = 0.0484, R_{sigma} = 0.0322]
Data/restraints/parameters	5020/1/317
Goodness-of-fit on F^2	1.067
Final R indexes [I>=2σ (I)]	R_1 = 0.0296, wR_2 = 0.0719
Final R indexes [all data]	R_1 = 0.0320, wR_2 = 0.0734
Largest diff. peak/hole / e Å^{-3}	0.90/-0.28
Flack parameter	0.017(9)

Table S8. Crystal data and structure refinement for complex 2 (obtained from DMF/Et_2O).

Identification code	complex 2 (DMF/Et_2O)
CCDC Number	**2368990**
Empirical formula	$C_{24}H_{35}N_7Ni_2O_2S_2$
Formula weight	635.13
Temperature/K	110.0
Crystal system	monoclinic
Space group	$P2_1$
a/Å	12.2300(7)
b/Å	9.0117(5)
c/Å	13.4991(8)
α/°	90
β/°	115.129(3)
γ/°	90
Volume/Å^3	1346.96(14)
Z	2
ρ_{calc}g/cm^3	1.566
μ/mm^{-1}	3.483
F(000)	664.0
Crystal size/mm^3	0.33 × 0.1 × 0.1
Radiation	CuKα (λ = 1.54178)
2Θ range for data collection/°	7.232 to 134.368
Index ranges	-13 ≤ h ≤ 14, -10 ≤ k ≤ 10, -16 ≤ l ≤ 16
Reflections collected	38955
Independent reflections	4744 [R_{int} = 0.0876, R_{sigma} = 0.0400]
Data/restraints/parameters	4744/1/336
Goodness-of-fit on F^2	1.074
Final R indexes [I>=2σ (I)]	R_1 = 0.0412, wR_2 = 0.0893
Final R indexes [all data]	R_1 = 0.0495, wR_2 = 0.0966
Largest diff. peak/hole / e Å^{-3}	0.56/-0.55
Flack parameter	0.023(14)

Table S9. Crystal data and structure refinement for complex 2 (obtained from MeOH/Et_2O)

Identification code	complex 2 (MeOH/Et_2O)
CCDC Number	**2379907**
Empirical formula	$C_{22}H_{32}N_6Ni_2O_2S_2$
Formula weight	594.07
Temperature/K	110.0
Crystal system	monoclinic
Space group	$P2_1$
a/Å	12.0943(4)
b/Å	9.0239(3)
c/Å	12.9900(5)
α/°	90
β/°	114.259(2)
γ/°	90
Volume/$Å^3$	1292.51(8)
Z	2
$\rho_{calc}g/cm^3$	1.526
μ/mm^{-1}	3.575
F(000)	620.0
Crystal size/mm^3	0.3 × 0.3 × 0.1
Radiation	CuKα (λ = 1.54178)
2Θ range for data collection/°	8.018 to 133.856
Index ranges	-14 ≤ h ≤ 14, -10 ≤ k ≤ 10, -15 ≤ l ≤ 15
Reflections collected	34921
Independent reflections	4583 [R_{int} = 0.0440, R_{sigma} = 0.0231]
Data/restraints/parameters	4583/1/248
Goodness-of-fit on F^2	1.074
Final R indexes [I>=2σ (I)]	R_1 = 0.0487, wR_2 = 0.1222
Final R indexes [all data]	R_1 = 0.0502, wR_2 = 0.1236
Largest diff. peak/hole / e $Å^{-3}$	1.50/-1.14
Flack parameter	0.32(4)

References

[29] Bruker (**2019**). *APEX3* (v2019.1-0) Bruker AXS Inc., Madison, Wisconsin, USA.

[30] G. M. Sheldrick, (**2016**). *SADABS.* University of Göttingen, Germany.

[31] G. M. Sheldrick, *Acta Crystallographica Section A* **2015,** *71* (1), 3-8.

[32] G. M. Sheldrick, *Acta Crystallographica Section C* **2015,** *71* (1), 3-8.

[33] O. V. Dolomanov, L. J. Bourhis, R. J. Gildea, J. A. K. Howard, H. Puschmann, OLEX2: a complete structure solution, refinement, and analysis program. *Journal of Applied Crystallography* **2009,** *42* (2), 339-341.

[34] C. F. Macrae, I. Sovago, S. J. Cottrell, P. T. A. Galek, P. McCabe, E. Pidcock, M. Platings, G. P. Shields, J. S. Stevens, M. Towler and P. A. Wood*, J. Appl. Cryst.,***2020**, *53*, *226-235*, 2020.

[35] P. R. Spackman, M. J. Turner, J. J. McKinnon, S. K. Wolff, D. J. Grimwood, D. Jayatilaka, M. A. Spackman, *Journal of Applied Crystallography* **2021**, *54*, 1006–1011.

DFT Optimized Coordinates for the OSS B3LYP Calculation for complex 1

28	-0.569658943	0.187098642	-0.402208859
28	-3.234865423	1.047060226	-0.035891586
17	-2.203072861	0.715764454	2.081215623
16	-1.413614369	2.068281075	-1.400462763
16	-2.352849184	-0.838273908	-1.405454191
7	0.961502964	1.373058785	0.340867521
7	-0.027936145	-1.672331941	0.339999699
7	-4.894477853	1.570570071	0.135676041
8	-5.934072912	1.888763224	0.585305159
6	1.983413846	1.491008372	-0.767552555
1	1.446885361	1.875530988	-1.636834218
1	2.290633682	0.473306767	-1.020337738
6	3.218567087	2.330663867	-0.486706155
6	0.763241713	-1.591884235	1.601147906
1	1.103492423	-2.598921933	1.872297720
1	0.071192655	-1.254434555	2.376603982
6	0.334872167	2.695390285	0.685105924
1	1.110675533	3.382843517	1.050408780
1	-0.362994858	2.484898360	1.496922992
6	1.237559791	-3.772700642	-0.486481894
6	1.951874850	-0.632754964	1.567365199
1	2.627990545	-0.852753785	0.734644334
1	2.537152946	-0.823204290	2.475279876
6	-1.311993143	-2.375158799	0.681323148
1	-1.754791060	-1.796063287	1.493101670
1	-1.088447284	-3.387662994	1.045658938
6	1.555747403	0.842221158	1.601134851
1	0.799159073	0.976896635	2.378034433
1	2.423961467	1.456073958	1.870894644
6	0.731890458	-2.367423355	-0.767602657
1	1.578741981	-1.724116179	-1.018536535
1	0.073636830	-2.363156049	-1.638210629
6	4.388799297	1.738996352	0.013391467

1	4.410655487	0.668586937	0.201878811
6	3.238241892	3.707026089	-0.758212433
1	2.358876634	4.184808664	-1.179747325
6	2.530661307	-3.981814097	0.017300570
1	3.176641210	-3.128643627	0.208481238
6	5.533274540	2.498536856	0.258201631
1	6.428130096	2.018132027	0.643161769
6	0.445783800	-4.897867631	-0.761418607
1	-0.545206552	-4.767662473	-1.185967280
6	-2.306324613	-2.426108853	-0.470683956
1	-3.299913568	-2.635121473	-0.066200885
1	-2.075891459	-3.216869740	-1.189990964
6	-0.441227378	3.323328661	-0.464517962
1	0.208950023	3.829390649	-1.183547363
1	-1.121588951	4.075494604	-0.057203808
6	4.379812751	4.471514088	-0.514080418
1	4.372559292	5.535056174	-0.733989070
6	3.009851812	-5.269029558	0.262493872
1	4.015064229	-5.406281684	0.650375408
6	5.529735773	3.870068388	-0.000434019
1	6.419749674	4.463563470	0.186599912
6	2.202032398	-6.376630143	0.000528450
1	2.573005763	-7.379932056	0.187889240
6	0.919726421	-6.187368894	-0.516905915
1	0.289724297	-7.043579112	-0.739472579

DFT Optimized Coordinates for the CSS B3LYP Calculation for Complex 1

28	-0.016180824	0.627378364	-0.305549201
28	-0.090648730	3.396553314	0.224914683
17	-0.060209485	2.219063290	2.294701897
16	1.454959257	2.102521405	-1.200575911
16	-1.560147899	2.023391562	-1.204802735
7	1.597906447	-0.451431187	0.374364827
7	-1.573200029	-0.533878306	0.371510764
7	-0.135285532	4.999817083	-0.155646583
8	-0.165243549	5.955454478	-0.820675225
6	2.050244942	-1.311382076	-0.786009590
1	2.232620536	-0.629274930	-1.617972779
1	1.192859887	-1.923946674	-1.073634184
6	3.253987794	-2.210929471	-0.557213388
6	-1.241971436	-1.326599362	1.590367137
1	-2.083295390	-1.992308669	1.818562866
1	-1.153128625	-0.607555581	2.408437709
6	2.639034225	0.554611825	0.781402197
1	3.541886311	0.027920542	1.120974947
1	2.205176573	1.098717778	1.622076845
6	-3.131381637	-2.381415087	-0.558321411
6	0.053615968	-2.128996444	1.514171286
1	0.070936593	-2.794412085	0.644864053
1	0.070019962	-2.790544223	2.388888329
6	-2.665904258	0.417311851	0.775570474
1	-2.262130577	0.984586634	1.615927933
1	-3.540628552	-0.154946480	1.114990556
6	1.306635203	-1.261798020	1.591870508
1	1.180617822	-0.549489728	2.410884042
1	2.180754329	-1.883824031	1.819996497
6	-1.978502779	-1.417756884	-0.788326990
1	-1.089432898	-1.983306925	-1.076187893
1	-2.197822047	-0.747079052	-1.620654824
6	3.086172464	-3.539069585	-0.135756722

1	2.084243649	-3.926579999	0.030609487
6	4.558413517	-1.756293727	-0.802935092
1	4.716506353	-0.744716318	-1.164734027
6	-2.890126771	-3.700746353	-0.145019752
1	-1.867925975	-4.034630574	0.014111506
6	4.183404223	-4.378648259	0.058702370
1	4.028343324	-5.403551712	0.383202227
6	-4.459760098	-1.996197297	-0.794371104
1	-4.674071835	-0.992644342	-1.149472909
6	-3.049504730	1.394917287	-0.322685391
1	-3.583445733	2.237491629	0.124004221
1	-3.710018009	0.952002920	-1.073565291
6	2.972993849	1.552936599	-0.314579991
1	3.658428699	1.146954846	-1.063921982
1	3.459828017	2.422176283	0.134820140
6	5.659434312	-2.591403859	-0.608999435
1	6.659778759	-2.218000628	-0.807631725
6	-3.939512366	-4.599174141	0.050564490
1	-3.727740145	-5.615934090	0.368570208
6	5.475444092	-3.904263049	-0.172727199
1	6.331468039	-4.555950911	-0.024767492
6	-5.256442685	-4.193733143	-0.171284378
1	-6.075363132	-4.891275156	-0.022380731
6	-5.513172260	-2.890313280	-0.599110510
1	-6.533266185	-2.570182883	-0.790151540

DFT Optimized Coordinates for the CSS TPSS Calculation for Complex 1

28	-0.000896982	0.643940988	-0.289905348
28	-0.004663228	3.322918724	0.203869333
17	-0.003014695	2.095931068	2.252683678
16	1.490722780	2.062364996	-1.213848137
16	-1.496278104	2.058102478	-1.214309278
7	1.574744576	-0.459348041	0.366541002
7	-1.573599336	-0.463638390	0.366322081
7	-0.007463477	4.965992179	-0.070069272
8	-0.009501707	5.982875913	-0.667251960
6	1.998950098	-1.327823698	-0.810568601
1	2.200305782	-0.632883126	-1.632783223
1	1.114993286	-1.908543949	-1.096706206
6	3.175228756	-2.264208470	-0.572702729
6	-1.272435678	-1.275736294	1.587905320
1	-2.139708172	-1.918226876	1.803920479
1	-1.160263368	-0.553944046	2.405723072
6	2.657150730	0.513817489	0.776548663
1	3.539708334	-0.051760720	1.118741851
1	2.229423374	1.076642229	1.613743791
6	-3.168725840	-2.273288083	-0.572812565
6	0.002730439	-2.115086316	1.497115728
1	0.003639535	-2.761072379	0.608327116
1	0.003600214	-2.795492369	2.360658475
6	-2.658680047	0.506634145	0.776146726
1	-2.232537133	1.070707728	1.613305346
1	-3.539722045	-0.061294485	1.118348228
6	1.275636317	-1.272319392	1.588044451
1	1.161435612	-0.550877093	2.405888826
1	2.144614153	-1.912477715	1.804136769
6	-1.995317635	-1.333325517	-0.810783383
1	-1.109674150	-1.911403808	-1.097086531
1	-2.198852778	-0.638954979	-1.632944167
6	2.960965708	-3.592727041	-0.154774606

1	1.941924222	-3.951204564	-0.007848396
6	4.501165672	-1.843388809	-0.793969617
1	4.693146802	-0.832933245	-1.152017781
6	-2.950278011	-3.601398113	-0.155762835
1	-1.930091972	-3.956924996	-0.009608175
6	4.034448124	-4.466458789	0.058182877
1	3.844710156	-5.489759078	0.378009083
6	-4.496034574	-1.856284007	-0.793082642
1	-4.691225735	-0.846189093	-1.150416803
6	-3.022955103	1.482183098	-0.332911508
1	-3.530701245	2.351011526	0.099856759
1	-3.686809179	1.046865652	-1.090284360
6	3.018872606	1.490484592	-0.332364416
1	3.683954712	1.057059363	-1.089737339
1	3.524223898	2.360640536	0.100541015
6	5.578370231	-2.712978681	-0.581090236
1	6.594837387	-2.367212647	-0.761194934
6	-4.021029279	-4.478448067	0.057295999
1	-3.828066415	-5.501361448	0.376430703
6	5.348286980	-4.025951257	-0.149471957
1	6.184803125	-4.703330257	0.012806606
6	-5.336290373	-4.041734794	-0.149362591
1	-6.170692455	-4.721698015	0.012991674
6	-5.570524861	-2.729203367	-0.580086736
1	-6.588119481	-2.386360783	-0.759410385

DFT Optimized Coordinates for the OSS TPSS Calculation for Complex 1

28	-0.016285833	0.643916805	-0.289751058
28	-0.083747711	3.321811934	0.203694789
17	-0.053057208	2.094949921	2.252620489
16	1.443416218	2.096294359	-1.211845233
16	-1.542586067	2.022907704	-1.216439078
7	1.583753792	-0.422948078	0.368410032
7	-1.563762528	-0.499680518	0.364967691
7	-0.130859028	4.964274210	-0.069986776
8	-0.169066264	5.980404973	-0.667242123
6	2.028467166	-1.281363883	-0.808395153
1	2.211444228	-0.582206360	-1.631343887
1	1.158968852	-1.884278621	-1.092875053
6	3.228559250	-2.187210270	-0.571273050
6	-1.245553892	-1.304432164	1.587050556
1	-2.097939714	-1.966959481	1.801823243
1	-1.151328824	-0.580267825	2.405047122
6	2.643504625	0.574346750	0.779423016
1	3.538637453	0.028692439	1.121274837
1	2.202835853	1.126629740	1.616908943
6	-3.112661473	-2.348983158	-0.574119463
6	0.048750639	-2.114142021	1.497743269
1	0.065162368	-2.760023232	0.609022830
1	0.064417586	-2.794266942	2.361363439
6	-2.670997214	0.445965406	0.773141106
1	-2.258260846	1.020571237	1.609890369
1	-3.539044206	-0.141443995	1.115697277
6	1.301914645	-1.242323201	1.589724896
1	1.170249387	-0.523437371	2.407198222
1	2.185150162	-1.862208760	1.807168632
6	-1.963771675	-1.379276131	-0.812335518
1	-1.063997718	-1.934924821	-1.099102644
1	-2.184883610	-0.690079751	-1.634300374
6	3.050001167	-3.517799311	-0.143180246

1	2.041144739	-3.900625982	0.012324979
6	4.542197563	-1.735081954	-0.803691863
1	4.706643949	-0.722669672	-1.169846038
6	-2.858747867	-3.673897333	-0.167239215
1	-1.829139902	-4.004747501	-0.029374892
6	4.146280110	-4.362939717	0.069035849
1	3.984110043	-5.388422534	0.396932619
6	-4.451261390	-1.963643672	-0.783646888
1	-4.673745905	-0.956375078	-1.132883869
6	-3.056696270	1.411629218	-0.337238510
1	-3.585747728	2.268424971	0.094018098
1	-3.708758615	0.960110498	-1.095439848
6	2.983350938	1.560017091	-0.328523581
1	3.659519079	1.142900967	-1.085172778
1	3.467379720	2.441613217	0.105602045
6	5.642083966	-2.576026122	-0.591756480
1	6.648476698	-2.206286650	-0.780597208
6	-3.905999782	-4.578802558	0.046152011
1	-3.685693694	-5.598674180	0.357212249
6	5.447452468	-3.891269022	-0.149773391
1	6.301566244	-4.546467230	0.011896942
6	-5.232934896	-4.173627541	-0.149749078
1	-6.049173409	-4.875216616	0.012904439
6	-5.502357571	-2.864474211	-0.570106352
1	-6.529241527	-2.545903009	-0.741024603

DFT Optimized Coordinates for the OSS B3LYP calculation on hypothetical monomeric [(dadt^{Bz})Ni•Ni(NO)(N$_3$)] complex

28	-0.486894721	0.105831371	-0.631389163
28	-3.156198923	0.684044850	-0.295428516
16	-1.462031557	1.864900912	-1.692382551
16	-2.100056973	-1.089473946	-1.694795436
7	0.837997344	1.453207241	0.224948733
7	0.158771500	-1.668916932	0.224874835
7	-4.841361052	1.044644436	0.037325193
8	-5.674454320	1.226445122	0.857533145
6	1.940858644	1.671905419	-0.786188600
1	1.451319777	1.990679618	-1.707892562
1	2.375254131	0.690478740	-0.991784111
6	3.050079728	2.638525236	-0.405294244
6	0.826153723	-1.485660676	1.544824688
1	1.233993930	-2.448958139	1.874616173
1	0.040391832	-1.200195083	2.248631265
6	0.036782814	2.698030673	0.485177487
1	0.685903130	3.466170244	0.929041787
1	-0.720361411	2.403726803	1.214824241
6	1.681591585	-3.663880098	-0.405711943
6	1.914791241	-0.416003725	1.584089994
1	2.675130861	-0.581323555	0.813920303
1	2.438885784	-0.530086682	2.540792866
6	-1.086386663	-2.469632512	0.484380478
1	-1.653867809	-1.887868004	1.213549416
1	-0.814486433	-3.437744027	0.928511922
6	1.368791034	1.009136855	1.544950642
1	0.535257728	1.075542249	2.248584867
1	2.139656789	1.716037436	1.875236067
6	1.071735343	-2.324936555	-0.786617334
1	1.873269385	-1.611419459	-0.992882879
1	0.493700842	-2.412647827	-1.707971563
6	4.232291030	2.170525767	0.188774067
1	4.353380067	1.106611166	0.376911936

6	2.943261544	4.011931204	-0.671650016
1	2.054941792	4.397884455	-1.162540561
6	2.952111578	-3.726897398	0.187030936
1	3.502773571	-2.808403775	0.374321619
6	5.264578473	3.045594814	0.528355979
1	6.171382979	2.659839654	0.985081171
6	1.015805271	-4.870056736	-0.671189166
1	0.046924689	-4.854062819	-1.161159784
6	-1.951788906	-2.660018394	-0.750086133
1	-2.946528996	-2.986300566	-0.435187831
1	-1.558932601	-3.422596439	-1.428340493
6	-0.672826890	3.230869876	-0.748252725
1	0.000484439	3.761326712	-1.427330934
1	-1.441360164	3.941190694	-0.432070128
6	3.972158522	4.891567373	-0.332842215
1	3.868356081	5.950510374	-0.550484687
6	3.530198907	-4.950587470	0.526218202
1	4.515857585	-4.974496952	0.981852613
6	5.134417264	4.411449909	0.272634083
1	5.936921473	5.095007286	0.533457975
6	2.846336301	-6.140236135	0.271360308
1	3.294419190	-7.094540257	0.531771255
6	1.588959107	-6.096520644	-0.332826654
1	1.056135758	-7.017656782	-0.549865555
7	-2.249385496	0.489107089	1.479437488
7	-2.894214687	0.625461007	2.503290799
7	-3.465026088	0.746172540	3.501416697

DFT Optimized Coordinates for the CSS TPSS calculation on hypothetical monomeric [(dadt^{Bz})Ni•Ni(NO)(N$_3$)] complex

28	-0.302695669	-0.552178737	-0.472898699
28	-1.944353299	-2.636964184	-0.024226793
16	-2.292496799	-0.781020004	-1.453495484
16	0.108260801	-2.501169158	-1.500055991
7	-0.937764475	1.244597796	0.255152174
7	1.582375253	-0.632174917	0.278777617
7	-3.232650965	-3.698468673	-0.026429746
8	-4.379948802	-3.963149698	0.100078879
6	-0.667825567	2.242466234	-0.866977244
1	-1.182049288	1.843574249	-1.747491631
1	0.406352796	2.183426716	-1.073452528
6	-1.063546854	3.688249218	-0.604004944
6	1.739383641	0.107015314	1.571401731
1	2.800402996	0.080552975	1.863805023
1	1.166824811	-0.459732783	2.314870641
6	-2.416134756	1.131012773	0.554064878
1	-2.794804322	2.118240027	0.867170754
1	-2.501451120	0.449811336	1.405412253
6	3.992887982	-0.062433473	-0.474163219
6	1.234450557	1.551111255	1.551127284
1	1.688321015	2.124580291	0.731215853
1	1.584365235	2.028068214	2.477677991
6	1.866121661	-2.084120615	0.592325034
1	1.140089067	-2.351538639	1.367905244
1	2.891549205	-2.173194275	0.988499370
6	-0.289796780	1.664451084	1.541138772
1	-0.705843158	1.022319020	2.328008794
1	-0.592569154	2.699474067	1.762189074
6	2.507213997	-0.093956273	-0.805183561
1	2.157856454	0.919125545	-1.032987519
1	2.306921409	-0.705327766	-1.691096667
6	-0.135971753	4.599678209	-0.061205301
1	0.876358483	4.264464186	0.165442534

6	-2.350067543	4.162563899	-0.926645085
1	-3.074348686	3.488418268	-1.382045437
6	4.580520368	1.091004808	0.082533876
1	3.964172565	1.970213868	0.271125789
6	-0.487336668	5.934396821	0.175576405
1	0.246426841	6.621608993	0.593481186
6	4.824913847	-1.166255067	-0.745509555
1	4.403315925	-2.057136343	-1.208750355
6	1.648356295	-2.991321834	-0.608631922
1	1.544452179	-4.025804686	-0.262816617
1	2.477485619	-2.959228213	-1.326441323
6	-3.210892556	0.587988167	-0.623087510
1	-3.408744796	1.349489701	-1.387265861
1	-4.176362032	0.208041770	-0.271318934
6	-2.706767394	5.496301878	-0.690650654
1	-3.706028965	5.841870127	-0.949759373
6	5.948069280	1.134357321	0.381150255
1	6.380770478	2.037645099	0.808046256
6	-1.777611982	6.384865728	-0.133716591
1	-2.053057773	7.422247609	0.047387401
6	6.757748254	0.020690270	0.121479353
1	7.821542112	0.052140199	0.350079325
6	6.192962509	-1.128328987	-0.447638496
1	6.817491678	-1.992224610	-0.668633160
7	-1.583408070	-1.456880075	2.574178309
7	-1.989719686	-0.837795929	3.491034467
7	-1.080940815	-2.062609502	1.646593924